

Dewatering Rock Crushing Fines Using Geotextile Tubes

by

William Scott Myers

A thesis submitted to the Graduate Faculty of
Auburn University
in partial fulfillment of the
requirements for the Degree of
Master of Science of Civil Engineering

Auburn, Alabama
May 14, 2010

Keywords: geotextile tubes, hanging bag tests, rock crushing fines

Copyright 2010 by William Scott Myers

Approved by

David J. Elton, Chair, Professor of Civil Engineering
Frazier Parker, Professor Emeritus of Civil Engineering
David H. Timm, Gottlieb Associate Professor of Civil Engineering
Raymond L. Powell, Assistant Director, NCAT

Abstract

A study on dewatering rock crushing fines using geotextile tubes was conducted. The laboratory portion included rapid dewatering tests and hanging bag tests to evaluate the dewatering efficiencies of the geotextiles as well as the use chemical flocculants. Settling ponds are currently the predominant method used to dewatering rock crushing fines. Settling ponds effectively dewater the material, but they are relatively slow and require large amounts of land.

Recent studies by Kutay and Aydilek (2005), Liao (2008), Liao and Bhatia (2005), and Kutay et al. (2005) have shown that geotextile tubes can be used to dewater high water content materials. These studies did not address dewatering rock crushing fines. Therefore the objective of this study was to assess the dewatering and filtration characteristics of geotextile tubes specifically for rock crushing fines. Tests showed that geotextile tubes effectively dewater rock crushing fines and retain the solid particles. The filter cake forming in the geotextile tube predominantly governs the filtration behavior. The chemical flocculants tested did not improve the dewatering efficiency or the filtration efficiency of the geotextiles.

Acknowledgments

First, I would like to give all credit to Jesus Christ, our Lord and Savior.

I would like to thank Dr. David Elton for his support and guidance from the beginning to the end of my masters program. He encouraged me to do my best at all times. I would also like to thank the rest of my thesis committee: Dr. Frazier Parker, Dr. David Timm, and Dr. Raymond Powell, for their encouragement, support, and hard questions.

I would also like to offer my thanks to the many people who donated materials and equipment that made it possible to conduct my research: Jason Jackson from Vulcan Materials, Peter Kaye from TenCate, Brian Mastin from WaterSolve, Jeff Fiske from Tensar International, Mike Groh from Geo-Synthetics, and Dr. Francisco Arriaga from the National Soil Dynamics Lab at Auburn University.

I am also grateful to Elliott Terrell and Brandon Johnson for assisting with the testing procedures. They were a great help and I appreciate all they did.

Lastly, I would like to thank my parents, Bill and Sandy Myers, for their continued support throughout my masters program and in everything I do.

Table of Contents

Abstract.....	ii
Acknowledgments.....	iii
List of Tables.....	viii
List of Figures.....	x
Chapter 1 - Introduction	1
1.1 – Background	1
1.2 – Purpose of this Study	1
1.3 – Research Approach.....	2
Chapter 2 – Literature Review.....	3
2.1 – Introduction.....	3
2.1.1 – Introduction to Geotextile Filtration.....	3
2.1.2 – Process of Geotextile Filtration.....	3
2.1.3 – Filtration Theory.....	4
2.2 – Existing Methods of Dewatering High Water Content Materials.....	6
2.2.1 – Ponds.....	6
2.2.2 – Belt Filter Press.....	7
2.2.3 – Geotextile Tubes.....	9
2.3 – Geotextile Fabric Characterization.....	12
2.3.1 – AOS.....	13

2.3.2 – Bubble Point Test Pore Size Distribution.....	13
2.3.3 – Wide Width Strength Test.....	14
2.3.4 – Seam Strength.....	14
2.3.5 – Water Flow Rate (Permittivity).....	15
2.3.6 – Ultraviolet Resistance.....	15
2.4 – Soil Characterization for Silts.....	16
2.4.1 – Mechanical Sieve Analysis.....	16
2.4.2 – Airjet Test for Grain Size Distribution.....	17
2.4.3 – Specific Gravity.....	18
2.4.4 – Particle Angularity.....	29
2.4.5 – Atterberg Limit.....	20
2.5 – Geotextile Filtration Tests.....	21
2.5.1 – Laboratory Test Methods.....	21
2.5.2 – Field Test Methods.....	27
2.6 – Geotextile Filter Failure Modes.....	31
2.6.1 – Clogging.....	31
2.6.2 – Blinding.....	34
2.7 – Characterization of Slurries and Effluent.....	35
2.7.1 – Total Suspended Solids Test.....	36
2.7.2 – Turbidity Test.....	36
2.7.3 – Visual Test.....	37
Chapter 3 – Experimental Approach.....	39
3.1 – Introduction.....	39

3.2 – Materials Evaluated.....	39
3.3 – Material Characterization.....	40
3.3.1 – Slurry Properties.....	40
3.3.2 – Geotextile Properties.....	45
3.3.3 – Polymers.....	53
3.4 – Laboratory Studies.....	53
3.4.1 – Consolidation.....	53
3.4.2 – Permeability.....	55
3.4.3 – Rapid Dewatering Test.....	57
3.4.4 – Hanging Bag Test.....	59
3.5 – Field Studies.....	63
3.5.1 – Moisture Content Studies.....	63
3.5.2 – Unit Weight Profiles.....	66
Chapter 4 – Results.....	69
4.1 – Material Characterization.....	69
4.1.1 – Slurry Properties.....	69
4.1.2 – Geotextile Properties.....	75
4.1.3 – Effect of Polymers.....	80
4.2 – Laboratory Studies.....	83
4.2.1 – Consolidation.....	83
4.2.2 – Permeability.....	87
4.2.3 – Rapid Dewatering Test.....	89
4.2.4 – Hanging Bag Test.....	93

4.3 – Field Studies.....	94
4.3.1 – Moisture Content Profiles with Moisture Probe.....	94
4.3.2 – Unit Weight Profiles.....	97
Chapter 5 – Conclusions.....	98
5.1 – Adequacy of Rapid Dewatering Test.....	98
5.2 – Adequacy of Hanging Bag Test.....	98
5.3 – Effect of Geotextile on Filtration.....	99
5.4 – Effect of Polymer on Filtration.....	100
5.5 – Water Content Variation in the Field.....	100
5.6 – Field moisture gauge results.....	100
5.7 – Consolidation Tests.....	101
Chapter 6 – Further Research.....	102
6.1 – Field Testing.....	102
6.2 – More Extensive Polymer Testing.....	102
6.3 – Predicting Geotextile Filtration Performance.....	103
References	104
Appendix 1	108
Appendix 2	113

List of Tables

Table 1 – Average Percent Passing	69
Table 2 – Average Air Jet Grain Size Distribution	71
Table 3 – Specific Gravity of Rock Crushing Fines	72
Table 4 – Water Content and Number of Blows for Liquid Limit Test.....	74
Table 5 – Geotextile AOS Comparison	76
Table 6 – Uniformity Coefficient from BPT	77
Table 7 – Wide Width Strength Test Comparison	78
Table 8 – Seam Strength Comparison	79
Table 9 – Water Flow Rate Comparison	79
Table 10 – Ultraviolet Resistance Comparison.....	80
Table 11 – Polymers Tested using RDT.....	80
Table 12 – Compression Index.....	84
Table 13 – Coefficient of Consolidation for Each Stress Increment.....	86
Table 14 – Air Jet Comparison Before and After Consolidation.....	86
Table 15 – Results of Permeability Testing	88
Table 16 – RDT without Polymer.....	89
Table 17 – RDT with Polymer.....	91
Table 18 – Results of HBT without Polymer	93
Table 19 – Results of HBT with Polymer.....	94

Table 20 – Calibration Testing for Field Scout TDR 30095

Table 21 – Chemical Composition of Polymers113

List of Figures

Figure 1 – Soil Arching	4
Figure 2 – Belt Filter Press	8
Figure 3 – Geotextile Tube	9
Figure 4 – Sample Grain Size Distribution	17
Figure 5 – Liquid Limit Device	20
Figure 6 – RDT Kit	22
Figure 7 – API Filter Press Apparatus	24
Figure 8 – Soil-Geotextile Permeameter	25
Figure 9 – Hanging Bag Test	28
Figure 10 – Geotube Dewatering Test	30
Figure 11 – Soil Retention Criteria of Steady-State Flow Conditions	33
Figure 12 – Hach 2100 AN Turbidimeter.....	37
Figure 13 – Rocks from Barin Quarry.....	40
Figure 14 – Geotextile Pore Size Distribution from the Bubble Point Test.....	48
Figure 15 – Constant Head Permeameter	56
Figure 16 – Rapid Dewatering Test Funnel.....	58
Figure 17 – Hanging Bag Test and Support Frame.....	60
Figure 18 – Modified Shelby Tube for Sampling Hanging Bag Test.....	62
Figure 19 – Field Scout TDR 300 Moisture Probe.....	64

Figure 20 – Field Scout TDR 300 Probes.....	64
Figure 21 – Water Content vs Period from Field Scout Calibration.....	65
Figure 22 – Field Scout TDR 300 Moisture Probe in use in the Field.....	66
Figure 23 – Balloon Density Apparatus.....	67
Figure 24 – Rock Crushing Fines Grain Size Distribution.....	70
Figure 25 – Air Jet Grain Size Distribution.....	71
Figure 26 – Crushed Rock Particles at 400x Magnification.....	73
Figure 27 – Liquid Limit Test.....	75
Figure 28 – Bubble Point Test Results.....	77
Figure 29 – Dewatering Efficiency of Solve 9310 at Varying Concentrations.....	81
Figure 30 – Comparison of Polymer Dewatering Efficiency at 0.006% Concentration.....	82
Figure 31 – Consolidation Strain vs Log Stress.....	83
Figure 32 – Consolidation Dial Reading vs Time for 5.99 kPa of Applied Stress.....	85
Figure 33 – Constant Head Permeability Test.....	87
Figure 34 – Permeability vs Density Results from Permeability Tests.....	88
Figure 35 - Percent Dewatered vs Initial Water Content from RDT Without Polymer.....	90
Figure 36 - Percent Dewatered vs Initial Water Content from RDT With Polymer.....	92
Figure 37 – Calculated Water Content vs Field Scout VWC.....	95
Figure 38 – Moisture Content Profiles from Barin Quarry.....	95
Figure 39 – Unit Weight Profiles from Barin Quarry.....	96
Figure 40 – Consolidation Dial Reading vs Time for 11.97 kPa of Applied Stress.....	108
Figure 41 – Consolidation Dial Reading vs Time for 23.94 kPa of Applied Stress.....	109
Figure 42 – Consolidation Dial Reading vs Time for 47.88 kPa of Applied Stress.....	109

Figure 43 – Consolidation Dial Reading vs Time for 95.76 kPa of Applied Stress.....110

Figure 44 – Consolidation Dial Reading vs Time for 191.52 kPa of Applied Stress.....110

Figure 45 – Consolidation Dial Reading vs Time for 383.04 kPa of Applied Stress.....111

Figure 46 – Consolidation Dial Reading vs Time for 766.08 kPa of Applied Stress.....111

Figure 47 – Consolidation Dial Reading vs Time for 1532.16 kPa of Applied Stress.....112

1. Introduction

1.1 Background

A total of 1.60 billion metric tons (Gt) of crushed stone was produced for consumption in the United States in 2007 (USGS, 2007). Crushing the stone generates dust which must be disposed of without polluting the surrounding environment. A common practice for quarries is to wash the rocks as they crush them and flush the slurry into settling ponds. At present, the most feasible way to dispose of these slurries is to hydraulically pump them into a dike-confined impoundment area and allow them to dewater by consolidation and desiccation. Then, the dewatered materials are taken to a landfill (Liao and Bhatia, 2005)

An alternative approach to dewatering the slurry created by crushing rock is to pump the slurry into geotextile tubes. The benefits of geotextile tubes include space savings because they can be stacked on top of each other creating a smaller footprint. The smaller footprint allows more rock to be mined. Geotextile tubes contain the slurry as it is drying to allow for easier removal once dry. The water exiting the tubes is generally clean compared to the influent. Therefore it will require little or no treatment before discharge into the local watershed.

However, it is still unknown how labor intensive geotextile tubes are compared to the common settling ponds. It is necessary to maintain the pumps used to pump the slurry into the tubes. Disposal of the dried slurry must also be considered.

1.2 Purpose of this Study

The purpose of this study was to determine the feasibility of using geotextile tubes to

dewater rock crushing fines. The evaluation of dewatering efficiency of geotextile tubes was done using rapid dewatering tests and hanging bag tests. The effect of polymers (chemical flocculants) on the dewatering process and characterization of the crushed rock particles was also evaluated.

1.3 Research Approach

In this study, two laboratory tests were conducted to evaluate the dewatering efficiency of geotextiles used in geotextile tubes. The test methods used were: Rapid Dewatering Tests (RDT) and Hanging Bag Tests (HBT)

The rapid dewatering test (RDT) is a test method developed by TenCate Geosynthetics to determine the geotextile filtration efficiency. The RDT can also be used to evaluate polymers effectiveness in speeding up the dewatering process.

The hanging bag test (HBT) is used to measure the dewatering efficiency of a geotextile. The HBT uses a large sample of 115 liters, compared to 500 ml for the RDT. The large sample size is a better estimate of field performance than the RDT and is much cheaper and easier to conduct than a full scale test.

Rock crushing fines from the Barin Quarry in Columbus, GA, were used to make the slurries that were dewatered by the geotextiles. Grain size distribution, permeability tests, compression tests, and specific gravity tests were conducted to characterize the quarry fines.

Bubble point tests were conducted to help characterize the geotextiles. Manufacturers' data were used for values of the geotextile apparent opening size (AOS), wide width strength, seam strength, permittivity, and ultraviolet resistance.

2. Literature Review

2.1 Introduction

2.1.1 Introduction to Geotextile Filtration

1. Separating soil and water

The purpose of a geotextile filter is to separate two mediums. For civil engineering applications this usually means separating soil and water. A perfect geotextile filter should allow all the water to flow out while retaining all the soil particles. This is impractical. If all the soil is retained, the water will not drain well. Conversely, if the filter allows all the water to come out easily, then it is hard to retain the soil particles.

2. Geotextile helps create a soil filter

A geotextile filter does not actually filter the soil, rather, it provides a barrier that allows the soil to form a soil filter at the geotextile and soil interface.

2.1.2 Process of Geotextile Filtration

At the geotextile and soil interface a phenomenon known as soil arching occurs. This phenomenon occurs when the soil particles form an arch, much like a bridge arch, that traps the soil particles that are behind the arch, keeping them from washing through the filter.

In order to ensure that soil arching occurs, it is necessary to choose a geotextile that has properties that are matched with the soil properties. No geotextile will filter all soils. Just like any cloth, geotextiles have a wide variety of holes, characterized by the apparent opening size (AOS) (ASTM D 4751). If the holes are too big, then the soil particles will flow through the geotextile

without arching and creating a filter. If the holes are too small, the soil particles will block the holes which clogs the geotextile and do not allow much water to pass through.

2.1.3 Filtration Theory

A. Soil Filtration

Soil arching is the process by which soil forms a filter to filter itself. Soil arching occurs when friction causes soil particles to form an arch and prevents piping. Piping is the erosion of soil particles through the geotextile. It is unlikely that soil arching will occur if there is not a proper grain size distribution. A well graded soil is desired, because it is more likely to form a soil arch. If the soil is poorly graded or gap graded, the likelihood of soil arching decreases significantly because the larger particles become locked together and prevent the smaller particles from passing through. See Figure 1.

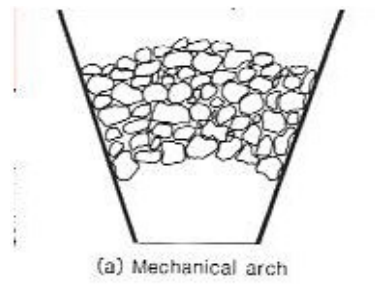


Figure 1: Soil Arching (Fasina, 2009 BSEN 7240 Notes)

B. Geotextile Filtration

1. Geotextile causes the soil to form a filter

The geotextile does not actually filter the soil, rather it is an aid to filtration. A geotextile filter causes the soil behind the geotextile to arch which actually filters the rest of the soil.

Therefore, a geotextile should be properly matched to the grain size distribution of a soil in order to ensure that soil arching occurs.

2. Geotextile properties needed

The apparent opening size (AOS) is a measure of the pore opening size of a geotextile. AOS is used to characterize geotextiles and is important when designing geotextile filters. The American Society of Testing of Materials (ASTM) test ASTM D 4751 determines the apparent opening size of a geotextile by dry sieving glass beads through a geotextile. Typically, ASTM D 4751 is used to characterize non-woven geotextiles. Dry sieving measures the nearly largest pore opening size (O_{95}) of a geotextile which indicates the approximate largest particle that would effectively pass through the geotextile (ASTM D 4751). That is considered to be the AOS (Aydilek et al, 2005). However, some of the problems associated with the AOS test are that the smaller pore opening sizes determined by this method may not be accurate due to various problems in the testing procedure. Also, this method does not determine the constriction size in the flow channels, which is the shape and size of the pore channels through the nonwoven geotextile (Aydilek et al, 2005).

Percent open area (POA) is used to characterize woven geotextiles. POA is a comparison of the open area of a woven geotextile compared to the area covered by the geotextile. This is accomplished by taking a known area of geotextile and determining the area covered by the geotextile and the area that is open and then dividing the open area by the total area.

The water flow through a geotextile is characterized by permittivity. Permittivity is defined as the cross-plane permeability coefficient divided by the thickness of geotextile at a specified normal pressure. It is American Society of Testing of Materials test designation ASTM D 4491 (Koerner, 2005). Permittivity is a function of geotextile thickness (Koerner, 2005) and, in general, thick geotextiles are expected to trap more soil particles than thin geotextiles due to their relatively

low permittivity. The permittivity of a geotextile may easily change during the dewatering process due to the intrusion of soil particles into the geotextile, especially in the presence of fine grained soils. (Kutay, et al, 2005) Therefore, permittivity may also be used to quantify the hydraulic performance of geotextiles after subjecting them to filtration with sludge in either lab tests, such as the Rapid Dewatering Test (RDT) or the gradient ratio test, or field tests. (Aydilek and Edil, 2002)

2.2 Existing Methods of Dewatering High Water Content Materials

2.2.1 Ponds

A. Pond Design and Operation

The purpose of a slurry pond is to allow the fine particles in the slurry to settle out. There are several different designs for slurry ponds, some impoundments are natural and some are man made while most are a combination. A typical slurry pond design takes advantage of the natural terrain using preexisting berms or hills to form part of the impoundment and building a man-made dam to close off the remaining portion. If the pond was never emptied it could cover several hundred acres and the confinement dams could reach heights exceeding one hundred feet. Therefore many quarries choose to empty their ponds frequently and dispose of the fine material elsewhere. It is necessary for the material to be dried in order to transport it by truck. Typically, the material should have a water content around 20% or less so that it will not liquefy when transported. The slurry is often placed in piles around the pond and allowed to dry under the sun.

B. Advantages

There are several advantages to using slurry ponds for dewatering rock crushing fines. One of the most appealing reasons for using a pond is that it is cheap compared to other methods. Slurry ponds are very reliable and have been used for a very long time. They always work.

C. Disadvantages

Ponds have disadvantages. Slurry ponds take up a lot of space that could be used for other purposes including mining underlying material. Ponds are very slow when compared to the belt filter press or geotextile tubes.

2.2.2 Belt Filter Press

Belt filter presses are used to remove water from liquid wastewater residuals and produce a non-liquid material referred to as “cake” (EPA, 2000). A belt filter press, also known simply as a belt filter, dewateres by applying pressure to the solids to squeeze out the water. Solids sandwiched between two tensioned porous belts are passed over and under rollers of various diameters. Increased pressure is created as the belt passes over rollers which decrease in diameter (EPA, 2000). Many designs of belt filtration are available, but all incorporate the following basic features: polymer conditioning zone, gravity drainage zones, low pressure squeezing zone, and high pressure squeezing zones shown in Figure 2.

A. Advantages

The advantages of a belt filter press are that it is much faster when compared to a settling pond or geotextile tube, and is very efficient at removing liquids (EPA, 2000). A settling pond may take several months to reach a low water content that can be achieved in less than a day using a belt filter press.

The belt filter press is a reliable machine for dewatering slurries. The staffing requirements are low, especially if the equipment is large enough to process the solids in one shift. Also, the maintenance is relatively simple and can be completed by the quarry maintenance crew (EPA, 2000).

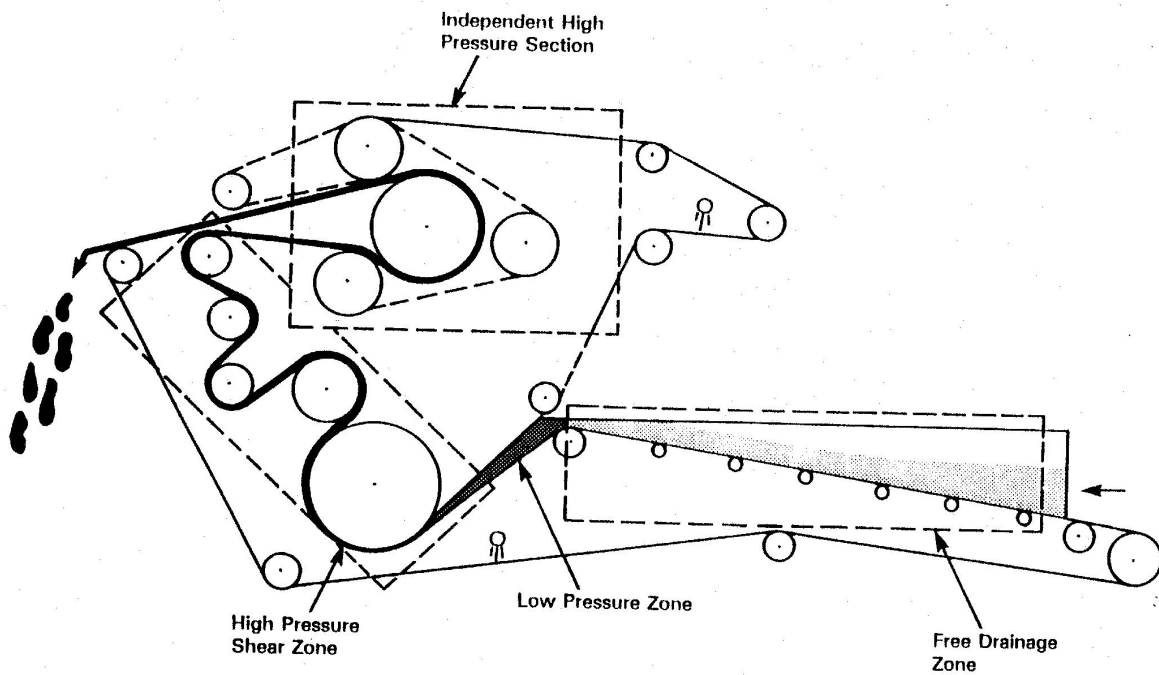


Figure 2: Belt filter press (EPA, 2000)

B. Disadvantages

A belt filter press is very expensive when compared to a settling pond or geotubes. This can be a major drawback, especially for small operations. The slurry solids must be screened and/or ground to minimize the risk of sharp objects damaging the belt (EPA, 2000). This should not be much of a problem when dewatering rock crushing fines because the pond slurry has a large percentage of solids passing the 0.075 mm sieve. Belt washing at the end of each shift, or more frequently, can be time consuming and require large amounts of water. An automatic belt washing system and the use of effluent reduces these costs (EPA, 2000).

2.2.3 Geotextile Tubes

Geotextile dewatering is the technique of separating solids and water in a sludge using geotextiles as the filter media (Muthukumaran, Ilamparauthi, 2006). A geotextile tube is a tube made out of a woven or nonwoven geotextile. Geotextile tubes can be made in a wide variety of sizes to meet the needs of the customer. According to Cantre (2002), geotextile tubes are filled hydraulically with a soil water mixture (slurry). The permeable tube enables the water to drain but retains the soil inside. Figure 3 shows a geotextile tube.



Figure 3: Geotextile Tube (Koerner, Koerner, 2006)

A. Design

The proper design of geotextile tubes requires that two phenomena take place simultaneously during dewatering, retention of solids in the geotextile tube and expulsion of water. If complete retention of solid particles occurs, generally not much water comes out. Conversely if a majority of the water comes out easily, usually the solid particles come out as well. Retention is affected by various parameters; the major factors being gradation of solids in the slurry, water content of the slurry, and opening size of the geotextile (Muthukumaran, Ilamparauthi, 2006). The permeability of

the geotextile should be considered as the permeability tends to decrease with time as the pores of the geotextile become clogged.

1. Filtration and Clogging

Geotextile tubes are designed in the same way as geotextiles for filtration and clogging. The tubes are designed to contain the solid particles while allowing liquid to escape. The ideal situation would be 100% retention of the solids while allowing liquids to quickly escape. The geotextile used to make the tube should be matched to the soil type to be filtered in order to ensure adequate dewatering while limiting piping, which is a loss of soil particles. If the geotextile pores are too small, the tubes clog quickly and the dewatering process becomes very slow. If the pores are too large, piping occurs.

2. Strength

A geotextile tube must also be designed to withstand the tensile forces which will be exerted upon it by the slurry during and after the filling cycle. It is very important that the tube be able to hold the slurry without bursting.

B. Advantages

According to Muthukumaran and Ilamparauthi (2006), geotextile tube dewatering is a technique having significant merits over the conventional disposal methods. Geotextile tubes used for dewatering high water content materials offer the advantages of rapid disposal of large volume of waste, ease of construction, convenient placement, high efficiency, low cost, labor savings, and low environmental impacts. Geotextile tubes are also efficient for separating and dewatering contaminated high water content waste.

1. Fast

Geotextile tubes are fast compared to settling ponds. The tubes can be brought to their final

height within a week or two depending on the material being dewatered and how quickly the dewatering occurs. According to a test run at the University of Georgia by Worley et al (2004) using lagoon slurry from a dairy lagoon, their geotextile tubes were filled five to six times at 2 to 5 day intervals and then allowed to dewater for an additional 2 weeks which allowed the desired water content to be reached (Worley et al, 2004). Comparatively, slurry ponds can take more than a month to dewater.

2. Space saving

Geotextile tubes can also be stacked to save space that would normally be used for a settling pond. This allows extra room for mining or other uses.

C. Disadvantages

1. Not common

As with many new ideas, geotextile tubes for dewatering of pond fines have not been readily accepted by the community. Geotextile tubes for use of dewatering pond fines are primarily being tested or researched by universities or the companies that make the tubes.

2. Somewhat unused/unproven

Sometimes clients are slow to begin using unused or unproven technology. This appears to be true for geotextile tubes. The quality of performance of geotextile tubes is not known and therefore this method is not commonly used by the firms who must dewater pond fines.

3. Non-reusable

Geotextile tubes must be disposed of after a single use, adding additional cost to the use of geotextile tubes.

D. Operation

1. Deployment

Geotextile tubes can be made in almost any size desired, from one to several meters in circumference and theoretically infinite in length. The ideal placement for geotextile tubes is on gently sloped ground with a 1% slope, this allows adequate drainage (Worley et al, 2004). A small, 15 – 20 cm, bed of stone or sand should be spread out as a footing and as a drain for the exiting water so as to prevent erosion. As the tubes are filled, new tubes can be stacked on top to create more drainage room reducing the footprint of the operation (Geosynthetics, Aug-Sept 2006).

2. Filling cycle

The filling cycle of the tubes is dependent upon the type of material being dewatered. A coarse sandy material will drain much faster than a fine grained sand or silt. Therefore, the tube should initially be filled to capacity and the height of the tube should be monitored so that the tube does not obtain a “pancake” shape as it will be nearly impossible to refill if that occurs. Over the course of a few days the height of the tube will decrease again and then a refilling is necessary before the tube deflates too much. Three or four iterations will most often be acceptable depending on the size of the tube and the material being dewatered (Worley, Bass, and Vendrell, 2004).

3. Removal and disposal

Once the material has reached the desired water content it can be disposed of. To access the material the tubes are cut open and a backhoe or similar equipment can be used to move the dewatered material. The dewatered material can be taken to a landfill, disposed of on-site, or left in the tubes until needed if it cannot be moved immediately. Once emptied, the tubes themselves can also be disposed of in a landfill as they are non-toxic.

2.3 Geotextile Fabric Characterization

It is important to characterize geotextiles in order to compare one geotextile. Characterizing

geotextiles allows the designer to pick a geotextile that will adequately filter a soil. There are several tests that are used to characterize geotextile fabrics ranging from strength tests to measuring pore opening sizes and resistance to ultraviolet degradation.

2.3.1 AOS - ASTM D 4751

Apparent opening size (AOS) is a common method of categorizing geotextiles. AOS was discussed in Section 2.1.3.

One problem with using AOS to characterize a geotextile is that the output is a single value. Geotextiles, especially nonwovens, have varying pore sizes and the AOS may not adequately characterize the geotextile. AOS is more accurate for woven geotextiles because they have more uniform openings. Another problem with AOS is that the smaller pore opening sizes determined by this method may not be accurate due to various problems in testing procedure. Furthermore, this method does not determine the constriction size, or flow path, in flow channels. However, the method is widely used by the geosynthetic manufacturers because it is an American Society of Testing of Materials standard (Worley, Bass, and Vendrell, 2004).

2.3.2 Bubble Point Test - ASTM D 6767

The bubble point test is American Society of Testing of Materials (ASTM) standard test designation ASTM D 6767. The bubble point test is based on the principle that a wetting liquid is held in the continuous pores of the geotextile by capillary attraction and surface tension, and the minimum gas pressure required to force liquid from these pores is a function of pore diameter (ASTM D 6767). A fluid-wet geotextile will pass air when the applied gas pressure exceeds the capillary attraction of the fluid in the pore constriction (ASTM D 6767). By comparing gas flow

rates of both a wet and dry geotextile at the same pressures, the percentage of the flow passing through the filter pores larger than or equal to the specified size may be calculated from the pressure-size relationship. By increasing pressure in small steps, it is possible to determine the flow contribution of very small pores size increments by difference of the wet and dry runs (ASTM D 6767). Using this method a pore size distribution curve can be obtained. This is considered a better description of the filtration characteristics of a geotextile than the one-point AOS.

2.3.3 Wide Width Strength Test - ASTM D 4595

The wide width strength test is a test method that covers the measurement of tensile properties of geotextiles using a wide-width strip specimen tensile method (ASTM D4595). The wide width strength test is regulated by ASTM. To conduct the wide width strength test, a relatively wide specimen of 200 mm (8.0 in) is gripped across its entire width in the clamps of a constant rate of extension (CRE) tensile testing machine operated at a prescribed rate of extension, applying a longitudinal force to the specimen until the specimen ruptures. Tensile strength, elongation, initial and secant modulus, and breaking toughness of the test specimen can be calculated from the test (ASTM D 4595).

2.3.4 Seam Strength - ASTM D 4884

The test for geotextile seam strength is regulated by ASTM and designated D 4884. The test specimen is 200 mm wide by 200 mm long with the seam running through the center of the sample for thermally bonded seams. For a stitch seam the samples are 200 mm but the seam should be 250 mm (10 inches). The test is run by gripping the sample in the clamps of a tensile testing machine and applying a longitudinal force, at a prescribed rate of extension, to the specimen until the seam or

geotextile ruptures (ASTM D 4884).

2.3.5 Water Flow Rate (Permittivity) - ASTM D 4491

ASTM D 4491 are the ASTM standard test methods for water permeability of geotextiles by permittivity. These test methods cover procedures for determining the hydraulic conductivity (water permeability) of geotextiles in terms of permittivity under standard testing conditions, in the uncompressed state (ASTM D 4491). The two test procedures used are the constant head method and the falling head method.

For the constant head test, a head of 50 mm (2 in) of water is maintained on the geotextile throughout the test. The quantity of flow is measured versus time. The constant head test is used when the flow rate of water through the geotextile is so large that it is difficult to obtain readings of head change versus time in the falling head test (ASTM D 4491).

During the falling head test, a column of water is allowed to flow through the geotextile and readings of head changes versus time are taken. The flow rate of water through the geotextile must be slow enough to obtain accurate readings (ASTM D 4491).

2.3.6 Ultraviolet Resistance - ASTM D 4355

The ASTM standard test method for deterioration of geotextiles by exposure to xenon arc radiation, moisture, and heat is designated D 4355. This test is intended to induce property changes associated with end use conditions, including the effects of solar radiation, moisture and heat (ASTM D 4355). The test does not account for deterioration due to local effects such as pollution or salt water exposure. Five specimens of a geotextile for the machine direction, the direction in which the material was sewn woven or assembled, and for the cross machine direction are exposed in a

xenon arc device for each of the following times: 0 (control specimens), 150, 300, and 500 hours. The exposure consists of 120 minute cycles as follows: 90 min of light only at $65 \pm 3^\circ \text{C}$ uninsulated black panel temperature and $50 \pm 5\%$ relative humidity, followed by 30 min of light and water spray (ASTM D 4355).

After each exposure period, the specimens are subjected to a cut or ravel strip tensile test. The average breaking strength in each direction is compared with the average breaking strength in each direction of the control specimens. The percent strength retained is plotted versus exposure period to produce a degradation curve for the specimens from each direction (ASTM D 4355). The ultraviolet resistance is important for geotextile tubes because they are constantly exposed to sunlight and the elements.

2.4 Soil Characterization for Silts

2.4.1 Mechanical Sieve Analysis

Mechanical sieve analysis is the common method for finding the grain size distribution of soil. The standard test method for particle size analysis of soils is ASTM D 422 . This test method covers the quantitative determination of the distribution of particle sizes in soils (ASTM D 422). Sieve analysis can be used on particles that are larger than a 0.075 mm (No. 200) sieve. If the particles are smaller, another method must be used such as a hydrometer (ASTM WK11776) or Air Jet sieving. A sample size of 115 g should be used for cohesionless soils. The sample is placed on a set of sieves ranging from 2.0 mm to 0.075 mm. Several sieves should be used in order to obtain a more accurate gradation curve. Conduct the sieving operation by means of a lateral and vertical motion of the sieve, accompanied by a jarring action in order to keep the sample moving continuously over the surface of the sieve (ASTM D 422). After shaking the sample, the percent

retained on each sieve must be determined. Percent retained is found by dividing the percent mass retained on the sieve by the total mass. Once percent retained is found, then percent passing is calculated by subtracting the percent retained on the first sieve from 100, then for the second sieve subtract the percent retained from the percent passing the first sieve and so on. Figure 4 shows a sample grain size distribution.

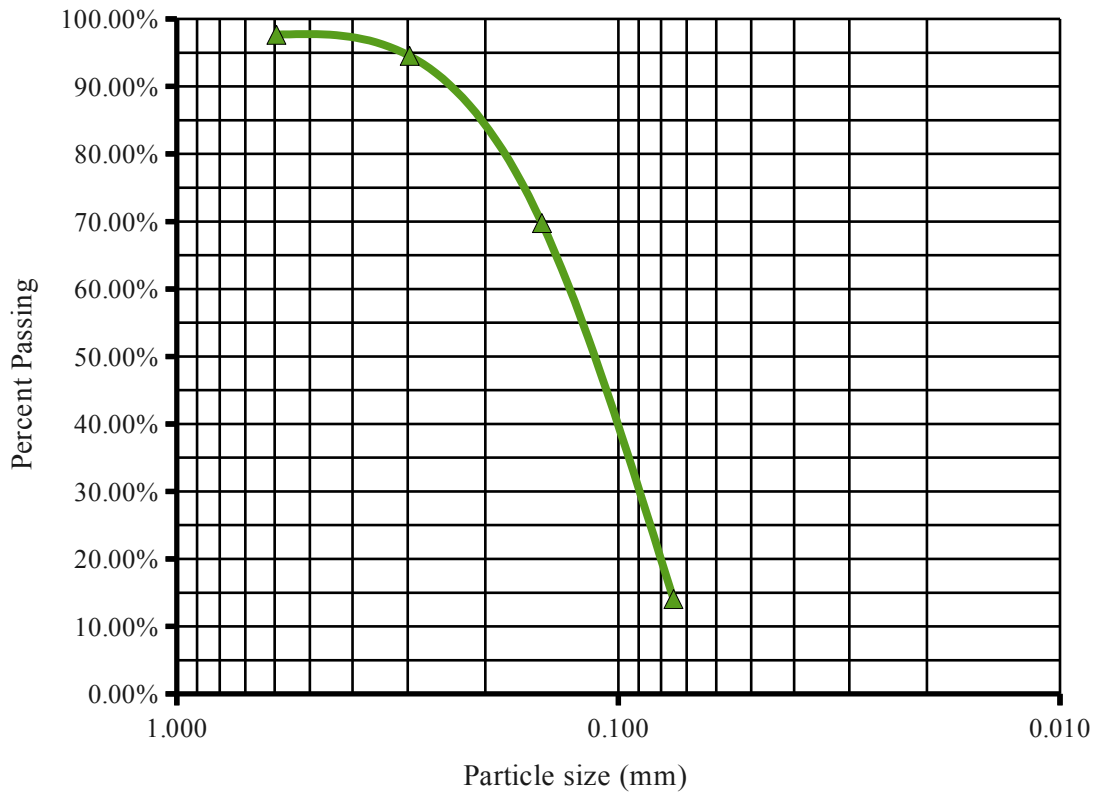


Figure 4: Sample grain size distribution

2.4.2 Air Jet Test for Grain Size Distribution - ASTM D 5158

ASTM D 5158 is the Standard test method for determination of particle size by Air Jet sieving. In the Air Jet test, a weighted sample of the material is placed in a test sieve that is inserted in the sieve holder of the Air Jet sieve assembly. Air is passed through the sieve from a slowly

rotating nozzle to fluidize the sample for a given period of time. Exit air flow removes undersized particles downward through the test sieve to a collection canister. The amount of sample retained on the test sieve is weighted and the percent passing the test sieve is computed by the difference. For a particle size distribution, the test must be repeated using sieves with different openings (ASTM D 5158).

2.4.3 Specific Gravity of Solids - ASTM D854

The specific gravity of soil solids is used to calculate the density of soil solids. The standard test method for determining the specific gravity of soil solids is ASTM D 854 . This test method is used to determine the specific gravity of soil solids that pass the 4.75 mm (No. 4) sieve, by means of a water pycnometer (ASTM D 854). To run the specific gravity test first one must calibrate the pycnometer, or volumetric flask. To calibrate the pycnometer the mass should be determined when it is dry, then it should be filled with water to the calibration mark on the pycnometer and weighed once again. The dry mass of the specimen to be tested should be 100 ± 10 g. Fill the pycnometer halfway with water and then pour in the dry soil and then the pycnometer should then be filled to the calibration mark with water. All the air should be removed from the soil in the pycnometer either by shaking or by a vacuum. Once the entrapped air is removed, the pycnometer with the soil and water is weighed. Pour out the slurry into a bowl of known weight and dry the soil completely and weigh again to determine the dry mass. Equation 1 shows the calculation of specific gravity:

$$G_s = \frac{M_s}{(M_{pw} - (M_{pws} - M_s))} \quad (1)$$

where,

G_s = Specific gravity of the solids

M_s = Mass of the oven dry soil solids (g)

M_{pw} = Mass of the pycnometer + water (g)

M_{pws} = Mass of the pycnometer + water + soil solids (g)

Determination of the specific gravity of soil solids is useful because the specific gravity is used in calculating the phase relationships of soils, such as void ratio and degree of saturation (ASTM D 854).

2.4.4 Particle Angularity

Angularity affects how easily particles will flow through a geotextile. Highly angular particles will have a tendency to be caught in the pores while a more rounded particle will flow through the pores. ASTM C 1252 is the standard test method for uncompacted void content of fine aggregate (as influenced by particle shape, surface texture, and grading) (ASTM C 1252). The test method covers the determination of the loose uncompacted void content of a sample of fine aggregate. When measured on any aggregate of a known grading, void content provides an indication of that aggregate's angularity, sphericity, and surface texture compared with other fine aggregates tested in the same grading (ASTM C 1252). A nominal 100 mL calibrated cylindrical measure is filled with fine aggregate of prescribed grading by allowing the sample to flow through a funnel from a fixed height into the measure. The fine aggregate is struck off and its mass is determined by weighing. Uncompacted void content is calculated as the difference between the volume of the cylindrical measure and the absolute volume of the fine aggregate collected in the measure (ASTM C 1252). The percent void content determined during the test depends on the particle shape and texture of a fine aggregate. An increase in void content indicates greater

angularity, less sphericity, or rougher surface texture, or a combination thereof (ASTM C 1252).

2.4.5 Atterberg Limits

The liquid limit and plastic limit are the Atterberg limits used in several engineering classification systems to characterize the fine grained fractions of soils. The plasticity index, PI, is the range of water content over which a soil behaves plastically. Numerically, it is the difference between the liquid limit and the plastic limit (ASTM D 4318). The liquid limit, plastic limit, and plasticity index of soils are also used extensively, either individually or together, with other soil properties to correlate with engineering behavior such as compressibility, hydraulic conductivity (permeability), compactibility, shrink-swell, and shear strength (ASTM D 4318).

The liquid limit is the water content of a soil at the arbitrarily defined boundary between the semi-liquid and plastic states. The liquid limit is determined by performing trials in which a portion of the specimen is spread in a brass cup, divided in two by a grooving tool, and then allowed to flow together from the shocks caused by repeatedly dropping the cup in a standard mechanical device shown in Figure 5 (ASTM D 4318).



Figure 5: Liquid Limit Device
(<http://www.wku.edu/~matthew.dettman/matt/prof/ce410/ll.htm>, 2009)

The liquid limit test uses 150 g of material at a known water content. The liquid limit can be estimated using Equation 2:

$$LL = W * \left(\frac{N}{25} \right)^{0.121} \quad (2)$$

where:

LL = liquid limit (%)

W = water content for the trial (%)

N = number of blows causing closure of the groove

The liquid limit, LL, is the average of two trial liquid limit values, to the nearest whole number without the percent designation (ASTM D 4318).

The plastic limit, PL, is the water content, in percent, of a soil at the boundary between the plastic and semi-solid states. The plastic limit is determined by alternately pressing together and rolling into a 3.2 mm diameter thread a small portion of plastic soil until its water content is reduced to a point at which the thread crumbles and can no longer be pressed together and re-rolled. The water content of the soil at this point is reported as the plastic limit (ASTM D 4318).

2.5 Geotextile Filtration Tests

2.5.1 Laboratory Test Methods

A. RDT Test

The Rapid Dewatering Test (RDT) is a quick and easy test procedure developed by Tencate to evaluate the efficiency of the candidate geotextiles and polymers used to dewater sludge (Tencate). The test requires a two piece funnel that holds the geotextile sample and the sludge,

shown in Figure 6.



Figure 6: RDT Kit

The sludge sample is then mixed with a polymer which aids in drainage and filtration by acting as a flocculant that clumps the solid particles together which enlarges the drainage paths allowing the water to flow more freely. The sludge and polymer mixture is then placed into the RDT test kit funnel, with the geotextile sample inserted between the two halves, and allowed to drain for 5 minutes. The effluent volume is measured every 30 seconds for 5 minutes to assess the efficiency of the geotextile and polymer in dewatering the sludge. The effluent is observed for clarity and can be quantified using either a total suspended solids test or turbidity test, which are explained in Section 2.7.1 and 2.7.2 respectively. A moisture content test is used to determine the percent solids, which is used to calculate the dewatering efficiency. The dewatering efficiency is calculated using

Equation 3:

$$DE = \frac{(PS_{final} - PS_{initial})}{PS_{initial}} \times 100 \quad (3)$$

where,

DE = Dewatering Efficiency

PS_{initial} = Initial percent solids

PS_{final} = Final percent solids

B. Filter Press Test

The filter press test, a standard test regulated by the American Petroleum Industry (API), typically is used to measure the filtration and wall-building properties of drilling fluids and cement slurries. However, it can also be used to test the filtration of slurries using geotextiles (API Filter Press Manual). The filter press test uses the apparatus shown in Figure 7. Once the sample is inserted into the machine, the desired pressure is applied for thirty minutes. During this time the effluent is collected in a graduated cylinder. The volume of filtrate collected in the graduated cylinder is measured and the filtrate loss in milliliters is recorded as the API (30 minute) filtrate loss of the slurry. The thickness of the filter cake is measured and recorded to the nearest 0.8 mm, (1/32") (API Filter Press Manual, 2009).

C. Gradient Ratio Test - ASTM D 5101

The gradient ratio test is used for evaluating the clogging of various soil-geotextile systems under controlled testing conditions (ASTM D 5101). The gradient ratio test can be performed on material that is smaller than 10 mm in diameter. A 1350 g soil sample is required for the test. The sample must be air dried for at least three days. Figure 8 shows a soil-geotextile permeameter used

for the gradient ratio test.

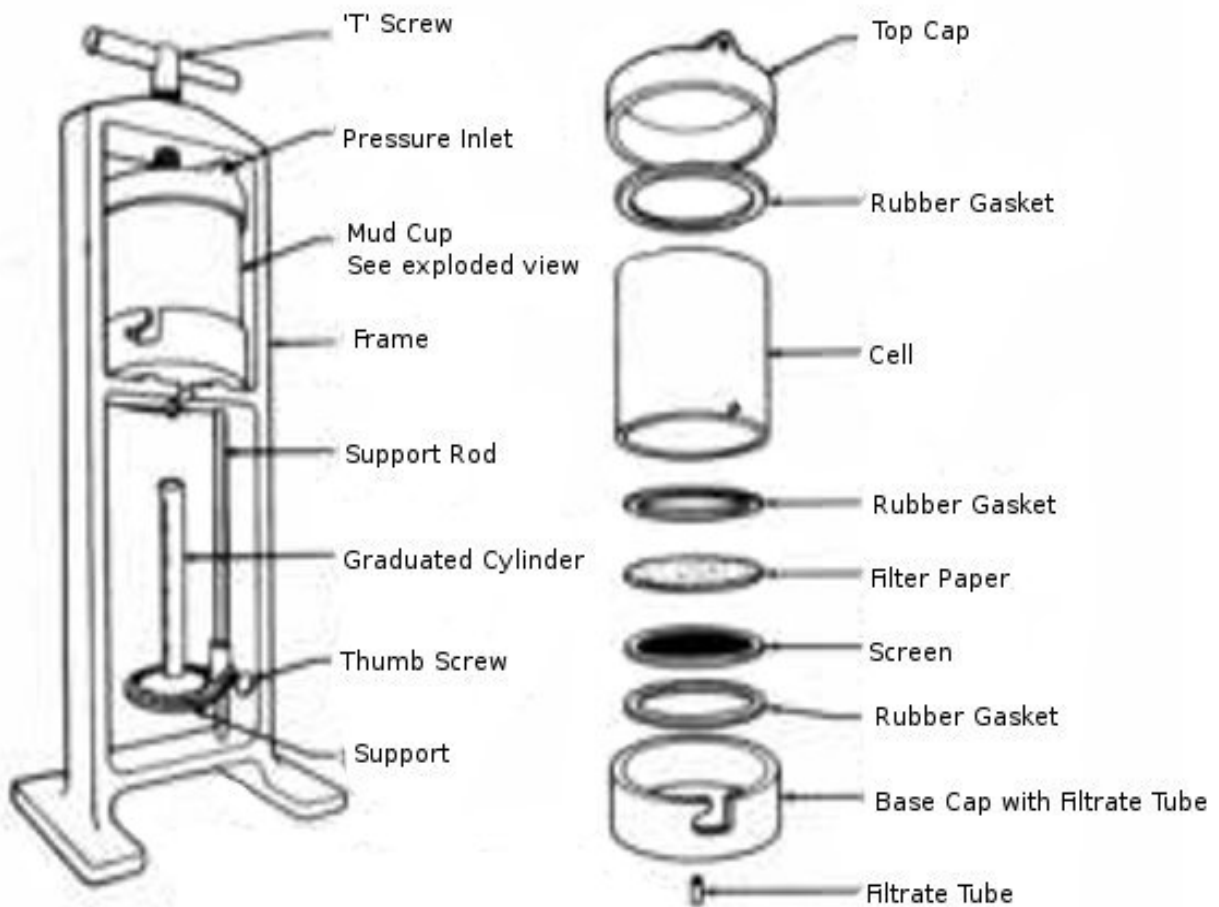


Figure 7: API Filter Press Apparatus (API Filter Press Manual)

Once the sample is prepared, the inflow to the system is adjusted so that a hydraulic gradient (i) of unity is obtained. Fluid flow through the system is begun and the data is recorded at 0, 0.5, 1, 2, 4, 6, and 24 hours from the initial starting time and every 24 hours thereafter until the system stabilizes. Stabilization is defined as the point where the flow rate and gradient ratio for three consecutive readings are within 10% of their apparent value (ASTM D 5101).

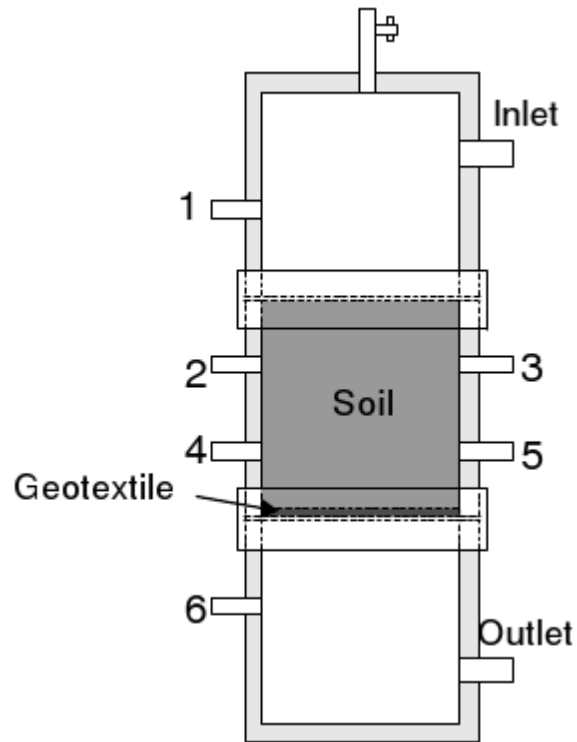


Figure 8: Soil-Geotextile permeameter (Kutay and Aydilek, 2003)

The flow rate from the system is recorded by measuring the time in seconds (t) for a measured quantity of flow (Q) in cubic centimeters for a minimum duration of 30 seconds and a minimum quantity of flow of 10 cm^3 (ASTM D 5101). The temperature (T) of the water in the system, measured in degrees Celsius, the water level readings from the individual manometers, and the date and time of day are also recorded. Once the system has stabilized, change the system hydraulic gradient to $i = 0.5$ and record the time. After $\frac{1}{2}$ hour at this level, record all data (ASTM D 5101). This process is repeated for $i = 5, 7.5,$ and 10 . Once the test has begun it cannot be stopped then resumed. It must run continuously (ASTM D 5101). The hydraulic gradient is calculated using Equation 4 (ASTM D 5101).

$$i = \frac{\Delta h}{L} \quad (4)$$

where,

Δh = difference between manometer readings for the soil zone between manometer 1 and manometer 6 (cm)

L = length or thickness of soil between the manometers being analyzed (cm)

The system permeability is calculated at the temperature of the test with Equation 5 and corrected to 20 degrees Celsius with Equation 6 (ASTM D 5101).

$$k_T = \frac{Q}{[(iAt) \times 100]} \quad (5)$$

$$k_{20} = \frac{k_T \mu_T}{\mu_{20}} \quad (6)$$

where,

k_T = system permeability at test temperature (m/s)

k_{20} = system permeability at 20°C (m/s)

Q = quantity of flow measured (cm³)

i = hydraulic gradient of the system

A = cross sectional area of the specimen (cm²)

t = time for the measured quantity of flow (s)

μ_T = water viscosity at test temperature

μ_{20} = water viscosity at 20°C

The gradient ratio, GR, is calculated using Equation 7.

$$GR = \frac{L_S \Delta h_{sf}}{L_{sf} \Delta h_s} \quad (7)$$

where,

$$\Delta h_s = \frac{(M_2 - M_4) + (M_3 - M_5)}{2}$$

$$\Delta h_{sf} = \frac{(M_4 - M_6) + (M_5 - M_6)}{2}$$

M_n = manometer reading for the manometer numbered n, see Figure 8 (cm)

L_s = 5.10 cm (Length of soil between manometer 3 and 5)

L_{sf} = 2.55 cm (Length of soil between manometer 5 and the geotextile)

D. Testing for filter cake retained on filter

Testing the filter cake, that is, the solid particles remaining on the filter after dewatering occurs, is another means of evaluating the efficiency of a geotextile and polymer for dewatering a particular sludge. The filter must be weighed before and after the filtration test is conducted. The filter must be dry before weighing. The weight of filter cake is determined by subtracting the initial filter weight from the final filter weight. The difference is the weight of solid particles trapped in the filter during dewatering. Determining the thickness or weight of the filter cake on the geotextile is necessary because two different polymers may allow the same amount of water through, but one polymer may reduce the filter cake on the geotextile which may reduce the filtration efficiency because of increased piping.

2.5.2 Field Test Methods

A. Hanging Bag Test

The hanging bag test was developed by the Geosynthetic Research Institute (GRI), with the cooperation of the member organizations for general public use (GRI - GT14). The hanging bag test is used for field assessment of fabrics used for geotextile tubes and containers and is a standard test method governed by GRI and designated GRI Test Method GT14. This test method is used to

determine the dewatering efficiency of dredged or slurried material passing through a geotextile bag. Results are quantitative in that the solids content of the slurry before and after dewatering can be determined, and qualitative in that visual observations of effluent and retained solids are made. The quantity of sediment that passes through the bag is also obtained (GRI - GT14). The hanging bag test is generally used to assess and decide on the appropriateness of a particular fabric to be used in the fabrication of a geotextile tube or container with respect to a site specific dredged or slurried material infill (GRI - GT14). Figure 9 shows a hanging bag test.



Figure 9: Hanging Bag Test

The standard test method for the hanging bag test is as follows: a geotextile bag is constructed by sewing one or more layers of fabric together to form a bag that will support and contain a measured amount of dredged or slurried material. Then the bag is suitably suspended from a support frame while the designated material is poured into it for the purpose of evaluation of the bag's filtration efficiency and effectiveness. This test is intended to be conducted in the field with in-situ dredged or slurried material. As such, the test is considered to be a performance test

(GRI). The final water content at the end of the HBT, influent and initial effluent percent solids, and effluent quality can be obtained from the HBT. The influent and initial effluent percent solids are measured at the beginning of the test. The final water content of the slurry is obtained when the test is finished, which occurs whenever water ceases to drain from the hanging bag. The effluent quality should be measured at 1, 10, and 30 minutes from the beginning of the test.

Some benefits of the hanging bag test are that it is conducted on site with in situ materials whereas the geotube dewatering test or RDT tests are typically conducted in a lab and the material must be transported to the testing location which allows the possibility of consolidation or evaporation. Also, the hanging bag test uses about 190 liters of material which gives a better assessment of what the actual field conditions will be. However, the hanging bag test does have some faults as well, namely that the flow conditions are vertical instead of horizontal and that the stress condition during filling are pulsed and low rather than continuous and high and therefore actual field performance may differ (GRI).

B. Geotube Dewatering Test from Tencate

The geotube dewatering test (GDT) is a demonstration of Geotube Dewatering Technology using 57 to 76 liter geotextile bags to visualize the dewatering process, evaluate the efficiency of the selected polymer, analyze clarity of the effluent, and predict achievable percent solids (TenCate). The GDT is a follow up test to the RDT test and is used to predict field performance of full scale geotextile tubes.

The slurry is mixed with the polymer in the predetermined dosage. The mixture is poured into the GDT bag to a known point on the stand pipe which indicates 6.9 kPa. The slurry is then allowed to dewater, either for a predetermined time or until the desired water content is reached. Effluent should be collected while dewatering is taking place and examined for clarity. Samples

may also be taken for testing if so desired (Tencate GDT). Figure 10 shows the GDT.



Figure 10: Geotube Dewatering Test (TenCate, 2009)

C. Full scale geotube test

Full scale geotextile tube tests are a means of determining the effectiveness of dewatering a slurry using a geotextile tube. All the other tests mentioned are indicators of what will happen in the field, but a full scale test is the only way to know for certain how effective geotextile tubes will be. Koerner and Koerner presented three case studies of field performance of geotextile tubes, summarized here.

Case no. 1 was utilizing geotextile tubes for shoreline protection transitioning from the beach to the boardwalk at a beach resort (Koerner and Koerner, 2005). The geotextile tube worked very well in this application. The sand within the tube dewatered quickly and the tubes were brought to final elevation within days of the start of construction. The tubes withstood both

Hurricanes Floyd and Isabelle and are still in place (Koerner and Koerner, 2005).

Case no. 2 was a project utilizing geotextile tubes for dewatering silts and clays that had silted up a marina. The geotextile tube worked poorly for this application as the dredged soil was very fine grained with a low permeability. Also, it had an oily consistency which caused rapid formation of a filter cake on the inside of the fabric. After formation of the filter cake, dewatering slowed considerably and the soil infill remained at a high water content (Koerner and Koerner, 2005). In order to remedy the situation, more tubes were needed to dewater the contracted amount of dredged material, and flocculants were also needed to improve the performance of the tube (Koerner and Koerner, 2005).

Case no. 3 was an industrial site. The geotextile tubes were utilized for dewatering lagooned ash. The material was classified as a well graded sandy silt, ASTM soil class SW (Koerner and Koerner, 2005). Depending upon who was interviewed, the geotextile tubes worked from good to fair for this application. The well-graded coarse ash within the tube dewatered at a steady rate, however, the tube did not reach a final moisture content of below 30% as originally anticipated (Koerner and Koerner, 2005). Some possible problems associated with this particular project were that the installation season was unusually wet and may have hampered dewatering. Also the strength of the tubes was insufficient to support stacking of the tubes and the layout of the project had to be changed (Koerner and Koerner, 2005).

2.6 Geotextile Filter Failure Modes

2.6.1 Clogging

A. Causes

1. Improper matching of geotextile to the soil

A geotextile must be designed to match the characteristics of the soil to improve the filtration and dewatering ability of the geotextile to reduce the probability of the geotextile becoming clogged. Clogging occurs when a geotextile becomes impregnated with soil particles. The soil particles block the drainage paths and can significantly reduce the dewatering capabilities of a geotextile. The most likely cause of clogging is a failure to properly design the geotextile, because clogging is a function of gradation (Koerner and Koerner, 2005). The intrusion of soil particles will affect the compressibility, filtration, and drainage characteristics of the geotextile (Palmeira and Gardoni, 2000).

2. Filter cake

The filter cake is a collection of soil particles on the surface of a geotextile and can also include soil particles impregnating the geotextile. The efficiency of the geotextile and the dewatering system can be greatly affected by the filter cake. According to Huang and Luo, the dewatering efficiency of the system can be greatly affected by the properties of the filter cake, such as its thickness and void ratio, rather than by the permittivities of the uncontaminated geotextile (Huang and Luo, 2007). Because the filter cake restricts water flow, it is important to estimate the permittivity of the filter cake as well. The permittivity of a filter cake is a function of its thickness and void ratio. A high void ratio and a small thickness correlates to a high permittivity, which is desired.

3. Clays and/or organics

Clays and organics can also increase the probability of clogging in a geotextile because clay particles and organic particles are more likely to be caught in the pores of the geotextile than non-cohesive silt or sand particles. Therefore, proper testing of a soil with a geotextile before full scale trials are begun is necessary to determine if a geotextile will be effective in dewatering the soil with

high clay or organic content.

B. Ways to reduce clogging

1. Proper design of the geotextile

Since clogging is a function of soil gradation (Koerner and Koerner, 2005), a geotextile should be properly designed to match the gradation of the soil being dewatered. This can be done by following the chart shown in Figure 11, developed by Luettich et al (1992) which takes into account soil type, gradation, and application requirements. The flow chart is read from left to right. The criteria depends upon particle size and whether permeability or retention is more desirable. Ultimately an O_{95} value is obtained, as described in Section 2.1.3. O_{95} is one of the major criteria for designing a geotextile. The O_{95} is used in geotextile filtration design procedures.

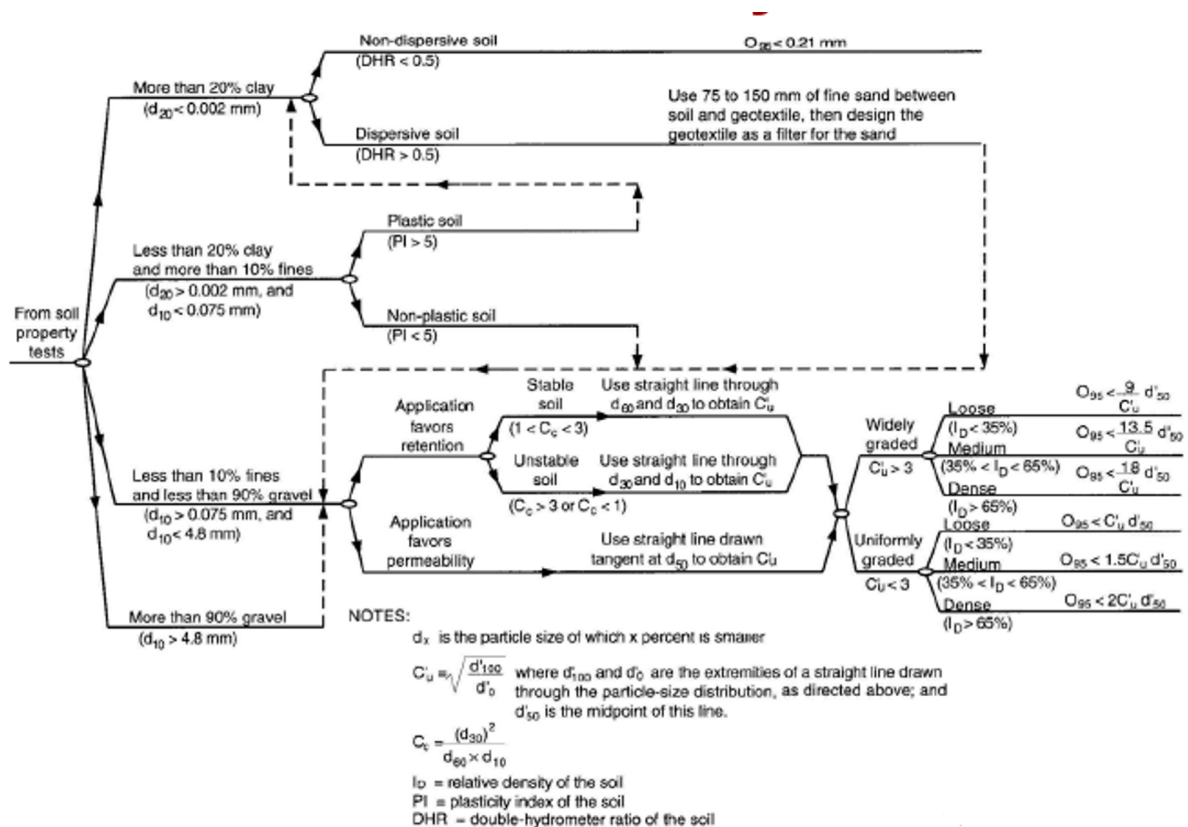


Figure 11: Soil Retention Criteria of Steady-State Flow Conditions (Luettich et al, 1992)

2. Increase porosity/permittivity of the geotextile

In addition to matching the geotextile pore size distribution to the soil grain size distribution, clogging can be reduced by increasing the permittivity of the geotextile. While this reduces the amount of clogging, increasing the permittivity also allows more piping, or erosion of soil through the geotextile, to occur, which is contrary to the purpose of a geotextile tube.

3. Add polymer to increase the porosity of the soil

Adding a polymer to the slurry is an effective means of reducing the amount of clogging that occurs. The polymer acts as a flocculant in the slurry which causes the soil particles to stick together, creating larger particles. This opens up the drainage path and allows more water to escape. The larger particles reduce the amount of clogging that occurs, since it is more difficult for larger particles to penetrate the geotextile.

2.6.2 Blinding - surface clogging

Blinding is the accumulation of soil particles on the surface of a geotextile. This phenomenon can be commonly seen in silt fences. As the silt washes down the hillside it is trapped by the silt fence and blinding occurs. Blinding covers up the pores, creating a low permeability layer. This is ideal for silt fences because the silt is allowed to settle out and the water slowly drains out leaving the silt behind. For geotextile tubes, however, blinding drastically decreases the effectiveness of the dewatering process.

A. Causes

1. Improper design of geotextile

Blinding can occur due to an improper design of the geotextile tube, which is caused by improperly matching the geotextile pore size distribution to the soil grain size distribution. To

reduce the probability of blinding, the Luettich chart (Fig. 11) should be used when designing a geotextile tube.

2. Clayey soils

Clayey soils are very likely to cause blinding because of their cohesiveness. The clay particles are likely to stick together and not pass through the geotextile. Instead they cake together on the surface of the geotextile preventing other particles and water from passing through.

B. Ways to reduce blinding

1. Proper design of geotextile

Proper design of the geotextile is one of the best ways to reduce blinding. It is necessary to decide if retention or permeability is the desired characteristic of the geotextile as different design criteria are applied to each. If the AOS and permeability of the geotextile can be properly designed to match the gradation of the soil to be dewatered, the likelihood of blinding is reduced. The process of designing geotextile filters is described in Section 2.1.3.

2. Addition of polymers to slurry

Addition of polymers to the slurry is an effective way to reduce blinding. The polymer acts as a flocculant in the slurry, joining soil particles together which creates larger particles. Larger particles have increased pore sizes between the particles which increases the permeability of the blinding layer allowing more water to flow through while still retaining the soil particles.

2.7 Characterization of Slurries and Effluent

Characterizing the effluent is an important step in determining the efficiency of a geotextile tube. The total suspended solids test (TSS), the turbidity test, and a visual test are used. The total suspended solids test actually measures the amount of solid particles in the effluent and is

a commonly used test for characterizing effluent. Turbidity is a measure of the light that is reflected while passing through a sample of effluent. A visual test involves looking at an effluent sample and making a judgment on the clarity of the sample.

2.7.1 Total Suspended Solids Test (TSS)

The Total Suspended Solids test (TSS) is a measure of suspended particles in an effluent. TSS is test 2540 D of the Standard Methods for the Examination of Water and Wastewater (1992). A well mixed sample is filtered through a standard glass-fiber filter of known weight and the residue retained on the filter is dried at 103 to 105°C to a constant weight. The increase in weight of the filter represents the total suspended solids (Standard Methods, 1992). Equation 8 was used to calculate TSS.

$$TSS \left(\frac{mg}{L} \right) = \frac{[(A - B) * 100]}{(sample\ volume, mL)} \quad (8)$$

where,

TSS = total suspended solids (mg/L)

A = weight of filter + dried residue (mg)

B = weight of filter (mg)

2.7.2 Turbidity Test

Turbidity is described in the Standard Methods for the Examination of Water and Wastewater Method 2130B (1992). Turbidity is an expression of the optical property that causes light to be scattered and absorbed rather than transmitted in straight lines through the sample (Standard

Methods, 1992). Modern turbidimeters, such as the Hach 2100 AN, shown in Figure 12, measure nephelometric turbidity units (NTU).

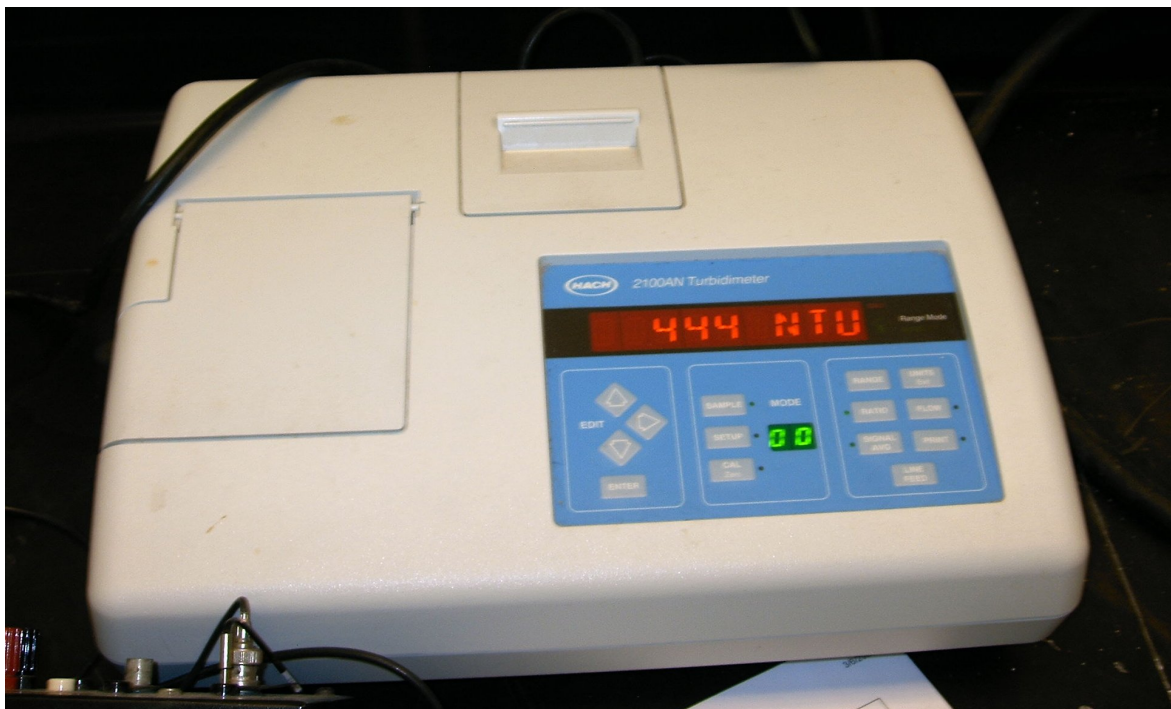


Figure 12: Hach 2100 AN Turbidimeter

The nephelometric method is based on a comparison of the intensity of light scattered by the sample under defined conditions with the intensity of light scattered by a standard reference suspension under the same conditions. An agitated 20 mL sample is placed into a turbidimeter while a light source illuminates the sample and photoelectric detectors indicate the intensity of light scattered at 90° to the path of incident light (Standard Methods, 1992). The test requires 15 seconds to complete and a readout is given in NTUs.

2.7.3 Visual Test

The visual comparison method is defined in Standard Methods test 2120 B and is a measure

of the color of the effluent. Color is determined by visual comparison of the sample with known concentrations of colored solutions. Comparison also may be made with special, properly calibrated glass color disks (Standard Methods, 1992). For examining slurry effluent, a 50 mL sample is compared to colored solutions of known concentrations, calibrated color disks, or other effluent samples.

3. Experimental Approach

3.1 Introduction

The rapid dewatering test (RDT) and hanging bag test (HBT) were used to determine the dewatering efficiency of the geotextile tubes. Consolidation and permeability tests were conducted on the slurry to help analyze the process that was occurring during dewatering. The slurry, geotextiles, and polymer were tested to better analyze the results from the lab tests. The slurry was characterized by water content, grain size, specific gravity, angularity, and Atterberg limits. These properties can affect the dewatering process and the choice of geotextile. The only test conducted on the geotextile was the bubble point test which gives a pore size distribution of the geotextile. The apparent opening size (AOS), the wide width strength, seam strength, permittivity, and ultraviolet resistance were taken from manufacturers' literature.

3.2. Materials Evaluated

The silt was obtained from Barin Quarry, in Columbus, GA operated by Vulcan Materials. The individual samples were prepared as described below. The geotextiles and polymers were obtained from manufacturers. The material needed for the bubble point and rapid dewatering tests were cut from samples sent by the manufacturers. The hanging bags were predominately pre-made by the manufacturers except for the bags made with the TenCate GT 500 material which were sewn together at Auburn University.

3.3 Material Characterization

3.3.1 Slurry properties

A. Geologic Composition

The rock mined from Barin Quarry is a granite, specifically a biotite gneiss. Biotite gneiss is a granitic gneiss in which the dominant mafic mineral is biotite (USGS, 2009). Mafic is simply a group of minerals rich in magnesium and iron (Merriam-Webster, 2009). Figure 13 shows the rock mined from Barin Quarry.



Figure 13: Rocks from Barin Quarry

B. Grain size distribution

The grain size distribution of the fines was determined using the standard test method for particle-size analysis of soils (ASTM D 422). This test method measured the distribution of particle sizes larger than $75\ \mu\text{m}$ (retained on the No. 200 sieve) (ASTM D 422). A large percentage of particles were smaller than $75\ \mu\text{m}$. Therefore, another method was needed in order to determine the size distribution of the smallest particles.

C. Air Jet sieving

Air Jet Sieving (ASTM D 5158) is designed to determine the size of activated carbon predominately smaller than a 180 μm (No. 80) sieve and, therefore, was ideal for determining the size distribution of the quarry fines that were smaller than 75 μm , or the No. 200 sieve (ASTM D 5158). The test is conducted by placing a sample of known weight in the sieve holder of the air-jet sieve assembly. Air is passed through the sieve from a slowly rotating nozzle to fluidize the sample for a given period of time. Exit air flow, provided by a vacuum cleaner, removes undersized particles downward through the test sieve to a collection canister. The particles retained on the test sieve are weighed and the percent passing the test sieve is computed by difference from the original weight. For a full particle size distribution curve, the test was repeated using sieves with different openings (ASTM D 5158).

D. Specific Gravity

The specific gravity of the material was found using the Standard Test Methods for Specific Gravity of Soil Solids by Water Pycnometer (ASTM D 854). This test method determines the specific gravity of soil solids that pass the 4.75 mm (No. 4) sieve, by means of a water pycnometer (ASTM D 854). The pycnometer was filled to the calibration mark with water and weighed to determine the mass of the pycnometer and water (M_{pw}). This was performed three times and the average taken. The soil was oven dried and the mass of the soil solids (M_s) was determined then poured into the pycnometer using a funnel. The pycnometer was filled with water until the level was half of the main body and it was covering the soil sample. The pycnometer was agitated until a slurry was formed and all soil that stuck to the sides was rinsed off. The sample was deaired using a combination of shaking and applying a vacuum. The pycnometer was then filled with water to the calibration mark used earlier and weighed once again to determine the mass of the pycnometer,

water, and soil solids (M_{pws}). The specific gravity of the soil solids was then determined using the following equation (ASTM D 854):

$$G = \frac{\rho_s}{\rho_w} = \frac{M_s}{\left(M_{pw} - (M_{pws} - M_s) \right)} \quad (9)$$

where,

G = specific gravity

ρ_s = density of the soil solids (g/cm^3)

ρ_w = density of water (g/cm^3)

M_s = mass of the oven dry soil solids (g)

M_{pw} = mass of the pycnometer and water (g)

M_{pws} = mass of the pycnometer, water, and soil solids (g)

E. Angularity

Angularity of soil particles can be determined using the Standard Test Method for Uncompacted Void Content of Fine Aggregate (ASTM C 1252). Void content provides an indication of an aggregates angularity, sphericity, and surface texture compared with other fine aggregates tested in the same grading (ASTM C 1252). To determine the void content of an aggregate, a 100 mL calibrated cylindrical measure is filled with fine aggregate by allowing the sample to flow through a funnel from a fixed height into the measure. The fine aggregate is struck off and its mass is determined by weighing. Uncompacted void content is calculated as the difference between the volume of the cylindrical measure and the absolute volume of the aggregate collected in the measure (ASTM C 1252). The uncompacted voids of an aggregate is determined

from Equation 10 (ASTM C 1252):

$$U = \frac{V - \left(\frac{F}{G}\right)}{V} \times 100 \quad (10)$$

where,

U = uncompacted voids in the material (%)

V = volume of cylindrical measure (mL)

F = net mass of fine aggregate in measure (g), total mass – mass of empty measure

G = dry relative density (specific gravity) of aggregate

A high uncompacted voids percentage indicates a highly angular particle. There is no direct measure of the angularity. Rather, several different soil samples, of the same size distribution, are compared against each other. Angularity of a soil is indicated relative to similar soils.

F. Atterberg Limits

The liquid limit, plastic limit, and plasticity index of soils are known as the Atterberg Limits. These limits can be found using the procedures in ASTM D 4318. The liquid limit is the water content, in percent, of a soil at the arbitrarily defined boundary between liquid and plastic states. The liquid limit is tested using a liquid limit device which consists of a brass cup suspended from a carriage designed to control its descent onto a hard rubber base (ASTM D 4318). Place a soil sample at a known water content in the cup. A groove should be made through the center of the sample using the tool provided with the liquid limit device. Then the number of drops required to close the gap 1.27 cm should be recorded. At least three samples should be used; the first with a water content that requires 25 to 35 drops to close the gap, the second with a water content that

requires 20 to 30 drops to close, and the third with a water content requiring 15 to 25 drops to close the gap. A plot of water content versus the corresponding number of drops is made. The water content corresponding to 25 drops is the liquid limit (ASTM D 4318).

The plastic limit is defined as the water content, in percent, of a soil at the boundary between the plastic and semi-solid states (ASTM D 4318). The plastic limit is found by taking a soil sample of 20 grams or more that has been dried to a consistency at which it can be rolled without sticking to the hands. This test is done by hand. The sample should be rolled between the hands into a cylindrical shape until its diameter reaches 3.2 mm. Once the desired diameter is reached the cylindrical thread should be broken into pieces and each piece should be balled up and rerolled into a thread having a diameter of 3.2 mm. Continue this process until the threads begin to crumble at 3.2 mm diameter, then collect at least 6 grams of the material and determine the water content (ASTM D 4318). The measured water content is the plastic limit.

The plasticity index is the difference between the liquid limit and the plastic limit. It is the range of water contents over which a soil behaves plastically (ASTM D 4318). The equation for the plasticity index is:

$$PI = LL - PL \quad (11)$$

where,

PI = Plasticity Index

LL = Liquid Limit

PL = Plastic Limit

3.3.2 Geotextile properties

A. AOS

Apparent opening size (AOS) is found using ASTM D 4751, the Standard Test Method for Determining Apparent Opening Size of a Geotextile. The AOS is determined by sieving glass beads through a geotextile. The geotextile is placed in a sieve frame, and glass beads, all of the same size, are placed on the geotextile surface. The geotextile and frame were shaken laterally to induce the beads to pass through the geotextile. The total weight of the glass beads used and the mass of the glass beads that pass through the geotextile are recorded to find the beads passing through the specimen.

$$B = \frac{100 * P}{T} \quad (12)$$

where,

B = beads passing through the specimen (%)

P = mass of glass beads in the pan (g)

T = total mass of glass beads used (g)

The procedure is repeated with various size beads until the AOS is determined. The AOS is size designation in millimeters of the beads of which 5% or less pass through the geotextile (ASTM D 4751). The test to determine AOS was not run for this research project; rather the values from the manufacturers were used.

B. Bubble Point Test

The Standard Test Method for Pore Size Characteristics of Geotextiles by Capillary Flow Test (ASTM D 6767) is more commonly known as the bubble point test. This test method is used to

determine the pore size distribution of geotextile filters with pore sizes ranging from 1 to 500 μm . The test method measures the entire pore size distribution in terms of a surface analysis of specified pore sizes in a geotextile, defined in terms of the limiting diameters (ASTM D 6767). The theory behind the bubble point test is discussed in Section 2.3.2

The bubble point test is conducted by placing a 4.60 cm diameter geotextile sample into a holder. Low air pressure is introduced (138 kPa (20 psi)) to the apparatus and the cutoff valve for the smallest rotometer, a device used to measure gas flow, is opened fully. Then the smallest metering valve is opened slowly, allowing air to pass through the first rotometer and the sample. When the air flow stabilizes, the rotometer value (airflow), the backpressure value, and the manometer value (pressure difference across the sample) are recorded (Elton et. al, 2007). Data points are initially recorded every 2 to 10 mm of water change in the manometer with increments of up to 100 mm or more used for the highest airflows. This procedure is conducted twice, once with a dry sample and once with a sample saturated with mineral oil. The calculation of pore size is based on the equilibrium of forces as shown in Equation 13 (ASTM D 6767):

$$\pi dTB \cos(\theta) = \left(\frac{\pi}{4}\right) d^2 P \quad (13)$$

where:

d = pore size (mm)

T = surface tension (mN/m or dynes/cm)

P = pressure (Pa or cm Hg)

B = capillary constant

θ = equilibrium contact angle

The left hand side of the equation is the resisting force developed from surface tension acting

between the liquid and the sidewalls of a pore constriction of diameter d . The right hand side is the driving force developed from the applied pressure multiplied by the area of the pore constriction (ASTM D 6767). Solving for d gives Equation 14:

$$d = \frac{4TB(\cos\theta)}{P} \quad (14)$$

The flow rate is found using Equation 15 (Elton et al, 2007):

$$Q_2 = Q_1 \sqrt{\frac{P_B + 14.7}{14.7}} \quad (15)$$

where:

Q_2 = true flow (L/min)

Q_1 = indicated flow (L/min)

P_B = reading from backpressure gage (psig)

The percent finer is calculated using Equation 16:

$$\text{Percent Finer} = \left(1 - \frac{Q_{2,w}}{Q_{2,D}} \right) * 100 \quad (16)$$

where:

$Q_{2,w}$ = true airflow from the wet run (L/min)

$Q_{2,D}$ = true airflow from the dry run (L/min)

The results are plotted on a semi-log graph of the percent finer versus pore size. The entire test and data reduction requires approximately one hour to complete (Elton et al, 2007). Figure 14 shows a plot of the pore size distribution of a geotextile from the bubble point test.

**PORE SIZE DISTRIBUTION
GT 500 (TenCate) 2008-08-26**

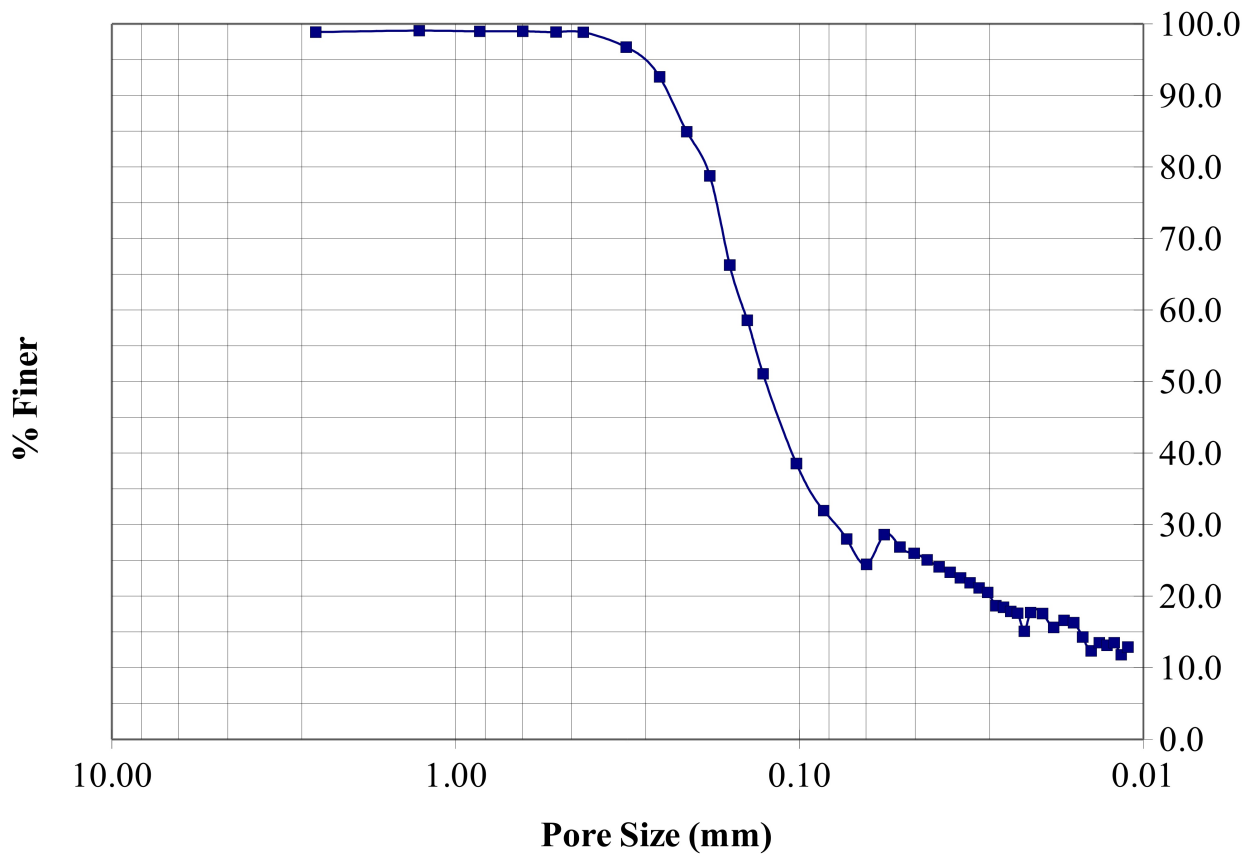


Figure 14: Geotextile pore size distribution from the bubble point test

C. Tensile strength

The wide width tensile strength test measures the tensile and elongation properties of geotextiles (ASTM D 4595). A relatively wide specimen (200 mm) is gripped across its entire width in the clamps of a constant rate extension type tensile testing machine operated at a prescribed rate of extension, applying a longitudinal force to the specimen until the specimen ruptures. Tensile strength, elongation, initial and secant modulus, and breaking toughness of the test specimen can be calculated from machine scales, dials, recording charts, or an interfaced computer (ASTM D 4595).

Because geotextile manufacturers generally perform this test and provide the information to the consumer, the wide width strength test was not conducted as part of this research experiment.

Wherever the wide width strength test was needed, the manufacturer's data was used.

D. Seam Strength

Seam strength of a geotextile is measured using the Standard Test Method for Strength of Sewn or Thermally Bonded Seams of Geotextiles (ASTM D 4884). This test method determines the seam strength of a geotextile that is 200 mm wide. The seam can be either sewn together or thermally bonded. The test is conducted by gripping a seam, 200 mm wide, across its entire width of the clamps in a constant rate of extension tensile testing machine, operated at a prescribed rate of extension, and applying a longitudinal (perpendicular) force to the specimen until the seam or geotextile ruptures (ASTM D 4884). The results of this method can be used for design of a geotextile to ensure that the geotextiles do not rupture under the working load.

ASTM D 4884 uses a wider sample than Test Method D 1683 and provides results that can more accurately correlate to the seam strength values anticipated in the field. The narrower test specimens have a tendency to contract (neck down) in the gage area, the area between the clamps, when under stress (ASTM D 4884).

The tensile strength of the seam is calculated using Equation 17 (ASTM D 4884):

$$S_f = \frac{F_f}{W_s} \quad (17)$$

where:

S_f = seam strength (kN/m)

F_f = observed breaking force (kN)

W_s = specified specimen width (m)

The seam efficiency is calculated from Equation 18 (ASTM D 4884):

$$E = 100 \times \left(\frac{S_b}{F_b} \right) \quad (18)$$

where:

E = seam efficiency (%)

S_b = seam breaking load (kN/m)

F_b = geotextile breaking load from ASTM D 4595 (kN/m)

Since the geotextile manufacturers conduct this test and provide the results, this test was not conducted as part of this research project. All values for seam strength were obtained from the manufacturer's data that was provided.

E. Water flow rate (permittivity)

The Standard Test Methods for Water Permeability of Geotextiles by Permittivity (ASTM D 4491) covers the procedures for determining the hydraulic conductivity (water permeability) of geotextiles in terms of permittivity under standard testing conditions, in the uncompressed state. Permittivity is an indicator of the quantity of water that can pass through a geotextile in an isolated condition (ASTM D 4491). Two tests can be used; a constant head test with a head of 50 mm (2.0 in) of water where the quantity of flow is measured over time, and the falling head test in which readings of head changes versus time are taken (ASTM D 4491). The constant head test is used when the flow rate of water through a geotextile is so large that it is difficult to obtain readings of head change versus time needed in the falling head test (ASTM D 4491).

The constant head test maintains a constant head of 50 mm (2.0 in) during the test period. Water is allowed to flow through the geotextile and the values of time and quantity of flow collected

from the discharge pipe are recorded (ASTM D 4491). Five readings should be taken for each specimen. Laminar flow is found by starting with a head of 10 mm and increasing the head by 5 mm until 75 mm is reached. Volumetric flow rate (Q/At) versus head should be plotted. The initial straight line portion of the plot defines the region of laminar flow; if the 50 mm head falls outside that region, repeat the test using the head of water that falls in the mid-region of laminar flow (ASTM D 4491). The permittivity can be calculated with Equation 19 (ASTM D 4491):

$$\psi = \frac{QR_t}{hAt} \quad (19)$$

where,

ψ = permittivity (s^{-1})

Q = quantity of flow (mm^3)

h = head of water on the specimen (mm)

A = cross-sectional area of test area of specimen (mm^2)

t = time for flow, Q (s)

R_t = temperature correction factor found using Equation 20

$$R_t = \frac{u_t}{u_{20C}} \quad (20)$$

u_t = water viscosity at test temperature (mP)

u_{20C} = water viscosity at 20°C (mP)

The falling head test is begun with a head of 150 mm and then the water supply is shut off and the water level is allowed to fall to 80 mm. The stop watch is started and the time for the water level to drop to 20 mm is recorded (ASTM D 4491). At least five readings should be taken per

specimen. The average permittivity is then calculated. Permittivity is calculated using Equation 21 (ASTM D 4491):

$$\psi = \left[\left(\frac{a}{At} \right) \ln \left(\frac{h_0}{h_1} \right) \right] R_t \quad (21)$$

where,

A = cross-sectional test area of specimen (mm²)

a = cross-sectional area of standpipe above specimen (mm²)

t = time for head to drop from h_0 to h_1 (s)

h_0 = initial head (80 mm)

h_1 = final head (20 mm)

R_t = temperature correction factor determined from Equation 20 above

The permittivity test was not conducted as part of this research project, because the data is provided by the manufacturers. Therefore, the manufacturer's values were used in any calculations requiring permittivity of a geotextile.

F. Ultraviolet Resistance

The Standard Test Method for Deterioration of Geotextiles by Exposure to Light, Moisture and Heat in a Xenon Arc Type Apparatus (ASTM D 4355) covers the determination of the deterioration in tensile strength of geotextiles by exposure to xenon arc radiation, moisture, and heat (ASTM D 4355). This method is intended to induce property changes associated with end use conditions, including the effects of solar radiation, moisture and heat (ASTM D 4355).

3.3.3 Polymers

Polymers were obtained from WaterSolve, LLC. Twenty four polymers were initially tested using the rapid dewatering test (RDT) to ascertain change in dewatering rates compared to RDT without polymer. All polymers were tested at the same concentrations and the six polymers causing the highest change in dewatering rates were selected for further testing at 0.3, 0.03, 0.006, 0.003, and 0.0015% by weight of slurry.

A breakdown of the chemicals in each polymer were obtained from the material safety data sheets (MSDS) provided by WaterSolve. This information was used to compare polymers and determine if there was a common ingredient in the most effective polymers versus the remaining ones.

3.4 Laboratory Studies

3.4.1 Consolidation

Consolidation testing was done according to the Standard Test Methods for One-Dimensional Consolidation Properties of Soils Using Incremental Loading (ASTM D 2435). This test method is the procedure for determining the magnitude and rate of consolidation of soil (ASTM D 2435). The soil specimen is restrained laterally and loaded axially with total stress increments. Each stress increment is maintained until excess pore water pressures are completely dissipated. During the consolidation process, measurements are made of change in the specimen height and these data are used to determine the relationship between the effective stress and void ratio or strain, and the rate at which consolidation can occur by evaluating the coefficient of consolidation (ASTM D 2435).

This procedure has several steps. A dry soil sample was placed into the provided cylinder

filled with water so as to ensure complete saturation of the sample. A porous filter stone was placed underneath the sample. The initial height of the sample was recorded and the porous stone was placed on top and the sample loaded into the consolidation device. An initial stress of 5.99 kPa was placed on the consolidation device and the deformation was recorded on a computer. Once the primary consolidation was finished and the deformation ceased, another stress of 11.97 kPa was loaded onto the device. Again the primary consolidation was allowed to take place and, once the deformation ceased, the stress was doubled. A total of nine stresses were applied, doubling each time, and the deformations measured as described. The stresses applied were 5.99, 11.97, 23.94, 47.88, 95.76, 191.52, 383.04, 766.08, and 1532.17 kPa.

The displacement of each stress was recorded and a graph of displacement versus time was constructed. The change in height was calculated using Equation 22:

$$\Delta = h_i - d \quad (22)$$

where,

Δ = change in height (mm)

h_i = initial height (mm)

d = measured displacement (mm)

The percent strain, which is the change in height divided by the initial height, was calculated with Equation 23:

$$\varepsilon = \frac{\Delta}{h_i} \times 100 \quad (23)$$

where,

ε = percent strain

The stress, which is force per unit area, was calculated using Equation 24:

$$\sigma = \frac{P}{A} \quad (24)$$

where,

σ = vertical stress (psi)

P = applied load (lbs)

A = cross sectional area of sample (in²)

Percent strain versus vertical stress was plotted to evaluate the compression index, C_c , and the preconsolidation pressure found using the Casagrande method.

The coefficient of consolidation indicates how rapidly or slowly the process of consolidation takes place (McCarthy, 2002) The coefficient of consolidation is found from Equation 25 (ASTM D 2435):

$$c_v = \frac{TH_{dr}^2}{t} \quad (25)$$

where,

c_v = coefficient of consolidation (cm²/s)

T = dimensionless time factor

t = time corresponding to the particular degree of consolidation (s)

H_{dr} = length of drainage path (cm)

3.4.2 Permeability

Permeability tests were conducted on the rock crushing fines to determine the coefficient of

permeability. ASTM D 2434 was used as a guideline. The constant head permeability test was used because the material tested is granular and there would be no change in hydraulic gradient. A permeameter, shown in Figure 15, was used to conduct the constant head test.



Figure 15: Constant head permeameter

A soil sample was placed in the cylinder with a porous stone and filter paper above and below. The weight of the soil was recorded to determine the density of the placement. The top plate was put in place and tightened. A vacuum pump was used to de-air the sample and slowly saturate the sample before the test was started. Once the sample was saturated, the inlet tube was filled with water and that level was maintained throughout the test. The head difference was measured as well as the length and cross sectional area of the specimen.

The inlet and outlet valves were opened to allow water to flow across the specimen. The effluent was captured in a graduated cylinder. Time and quantity of effluent were recorded to determine the coefficient of permeability using Equation 26 (ASTM D 2434):

$$k = \frac{QL}{Ath} \quad (26)$$

where,

k = coefficient of permeability (cm/s)

Q = quantity of water discharged (cm³)

L = length of specimen along path of flow (cm)

A = cross sectional area of specimen (cm²)

t = interval of time over which flow Q occurs (s)

h = difference in hydraulic head across the specimen (cm)

To achieve densities similar to in-situ conditions the samples had to be compacted. Dry rock crushing fines were placed into the permeameter in two inch lifts and compacted by hand with a dowel until the volume became constant. Successive lifts were placed in the same manner until the permeameter was full. Several tests were run at varying densities. The density was calculated from Equation 27:

$$\rho = \frac{m}{V} \quad (27)$$

where,

ρ = density (g/cm³)

m = dry mass of soil sample (g)

V = volume of soil sample (cm³)

3.4.3 Rapid Dewatering Test (RDT)

The rapid dewatering test (RDT) was developed by TenCate as a quick and easy test to

determine how well a slurry dewater through a geotextile sample (RDT Manual, 2009). The test is also used to determine the efficiency of polymers that accelerate the dewatering process.

A. RDT without polymer

The RDT uses a geotextile sample that is 9.5 cm in diameter. The sample is placed into the RDT funnel shown in Figure 16. A 500 mL slurry sample of known water content is poured into the funnel and allowed to dewater. The volume of effluent is recorded every 30 seconds for 5 minutes.



Figure 16: RDT Funnel (RDT Manual, 2009)

After 5 minutes, the slurry remaining in the funnel is placed in a bowl and the final water content is measured. The effluent can be tested to determine the total suspended solids (TSS) and/or the turbidity. The dewatering efficiency is calculated using Equation 28:

$$DE = \frac{PS_f - PS_i}{PS_i} \quad (28)$$

where,

DE = dewatering efficiency (%)

PS_f = final percent solids (%)

PS_i = initial percent solids (%)

TSS is found by weighing a pan and glass fiber filter, then filtering the effluent through the filter to catch all the particles, drying the filter, and finally weighing the pan and filter with dried sample after drying. TSS is calculated using Equation 29:

$$TSS = \frac{W_{p+f+s} - W_{p+f}}{V_E} \times 1000 \quad (29)$$

where,

TSS = total suspended solids (mg/L)

W_{p+f+s} = weight of pan + filter + dried solids (mg)

W_{p+f} = weight of pan + filter (mg)

V_E = volume of effluent (mL)

B. RDT with polymer

When using a polymer the only difference from the previously described procedure is the addition of polymer. A 1% solution of polymer is made up by combining 1 mL of polymer to 100 mL of water and thoroughly mixing. The solution should sit at least 15 min after mixing. The desired amount of polymer is then thoroughly mixed with the slurry. After mixing the polymer into the slurry, the slurry is poured into the RDT funnel. The procedure for measuring effluent, water content, and TSS is the same as when no polymer was used.

3.4.4 Hanging Bag Test (HBT)

The hanging bag test (HBT) is used to determine the dewatering efficiency of dredged or slurried material passing through a geotextile bag (GRI-GT14). The standard test method for the

Hanging Bag Test for Field Assessment of Fabrics Used for Geotextile Tubes and Containers was developed by the Geosynthetic Research Institute (GRI) and is designated GRI Test Method GT14 (GRI – GT14). The HBT uses bags that hold between 113 to 190 liters of slurry. The bags are simple to make from a rectangular piece of fabric folded in half with the edges sewn together with handles sewn at the top opening. The bags are turned inside out once sewn so that the side stitching is on the inside. A bag used for the test is shown in Figure 17:



Figure 17: Hanging Bag Test Bag and Support Frame

A. HBT without polymer

The HBT uses in-situ material and is a performance test meant to simulate field conditions when using a large geotextile tube (GRI - GT14). 113 liters of slurry for the HBT was mixed in five

gallon buckets for ease in handling. The slurry was mixed at a water content of 50% to better correlate with the RDT and also because that was approximately the water content of the in situ material. After thorough mixing, the buckets were poured as quickly as possible into the hanging bag. The test was begun when the last bucket was emptied into the bag. A one minute delay was typical between pouring the first bucket and the last. An initial effluent sample was taken immediately after the pouring was completed as well as an initial sample of the influent. The water content and percent solids of each sample were measured and used to determine the removal efficiency, which was calculated using Equation 30 (GRI - GT14):

$$\text{Removal Efficiency} = \frac{I_S - E_S}{I_S} \quad (30)$$

where,

I_S = Influent percent Solids (%)

E_S = Effluent percent Solids (%)

Effluent samples were collected at 1, 10, and 30 minutes and tested for total suspended solids (TSS) and turbidity as described in Section 2.7.1. Slurry samples were collected at times of 30 minutes, and 1, 2, 3, 4, and 24 hours. The slurry samples were taken using a modified Shelby sampling tube shown in Figure 18. The sampler was pushed into slurry and the handle was screwed into the top creating a seal. The sampler was extruded and the sample placed into a container for testing. The sampling procedure had to be conducted quickly as the material would not remain inside the sampler for longer than three to four seconds once the sampler was extracted from the slurry. Samples taken by the modified Shelby sampling tube did not retain a cylindrical shape if the water content of the slurry was greater than 35%, instead they conformed to the shape of the container. If

the water content was less than 35% the extruded samples would retain a cylindrical shape if not agitated.



Figure 18: Modified Shelby tube for HBT sampling

The GT14 test method states that the HBT should be stopped after liquid ceases to drain from the bag. Liquid ceased to drain around the 12 hour time period, but the test was extended to 24 hours to have a standard time with which to compare different geotextiles. Within 48 hours from the beginning of the hanging bag test, if the bags were agitated the water would flow again for a short period of time.

B. HBT with polymer

When a polymer was used, the only procedure that changed from that described above was the mixing. The polymer was mixed in at 0.006% by weight. To determine the volume of polymer

used in each bucket, Equation 31 was used:

$$Vol. Polymer (mL) = Wt. Soil (kg) \times 0.06 \quad (31)$$

The constant, 0.06, includes the conversion of 0.006% to a decimal value and converting kg to g. Because the specific gravity of the polymer used was 1, the weight, in grams, of polymer needed was numerically equal to the volume in mL. After the mixing process was completed, the procedure was conducted as stated above. The same sampling and evaluation procedures were used.

3.5 Field Studies

Moisture content and density studies were conducted to determine the in-situ properties of the quarry fines. The moisture content studies were conducted with a moisture probe that allowed instant readings of moisture content. Density measurements were obtained using a balloon density apparatus.

3.5.1 Moisture Content Studies

A Fieldscout TDR 300 moisture probe, shown in Figure 19, was used to conduct the vertical moisture content profiles of the piles of quarry fines. The Fieldscout has two built-in volumetric water content (VWC) calibrations, one for general soils and one for soils with high clay content. Before being used to measure field moisture contents at the quarry, the moisture probe was calibrated to ensure that the results obtained in the field were accurate.

The Fieldscout TDR 300 uses time domain reflectometry (TDR) to estimate the water content. TDR works on the same principle as radar. A pulse of energy is transmitted down two 20.1 cm metal rods, shown in Figure 20,



Figure 19: Field Scout TDR 300 moisture probe (Ben Meadows, 2009)

when the pulse reaches the end of the rods, part or all of the energy pulse is reflected back to the instrument (SOWACS, 2009). Soil and water impede the pulses of energy.



Figure 20: Field Scout TDR 300 probes (Professional Equipment, 2009)

Water has a high impedance compared to soil. A higher water content corresponds to a longer travel time. The time, or period, for the energy pulses to travel the length of the rod is measured by the Fieldscout TDR 300 in milliseconds and converted into VWC, which is presented as a percentage.

A. Moisture probe calibration

The Fieldscout TDR 300 was calibrated in the lab using the same soil that would be measured in the field. Several different soil samples were made up in the lab at different water contents and then volumetric water content and period readings were taken. The samples were dried overnight and the actual water content was calculated. The calculated water content was compared

to the readings from the TDR 300 to determine if a new calibration was necessary. A new calibration was not necessary for this soil. However, the calculated water content (%) can be plotted versus the period (ms) and the equation of the plotted line could be used to program the Fieldscout TDR 300 with a new VWC calibration if necessary. See Figure 21.

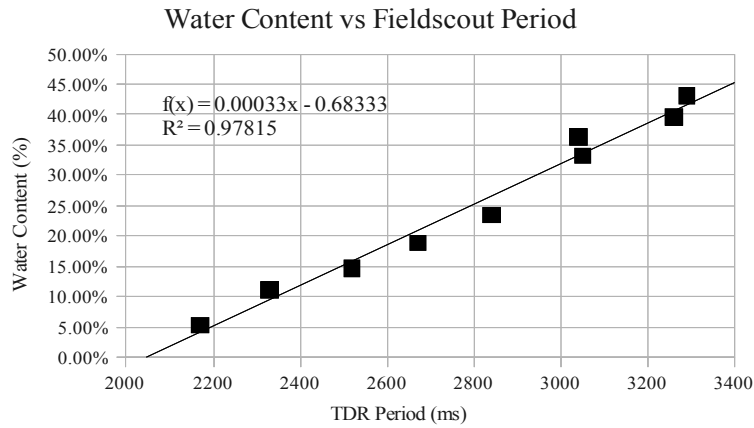


Figure 21: Water content vs period from Field Scout Calibration

B. Field vertical water content profiles

The in-situ vertical water content profiles, water content measurements taken from the top to bottom of the piles of rock crushing fines, were used to understand how the rock crushing fines drain. The Fieldscout TDR 300 was used to take readings, shown in Figure 22. Readings were taken starting from the bottom of the pile to the top in 0.9 meter increments. Three readings were taken at each location and the average of the three readings was taken as the water content in that location.



Figure 22: Fieldscout TDR 300 moisture probe in use in the field

3.5.2 Field unit weight profiles

In-situ unit weight, or density, profiles of the piles of rock crushing fines were conducted using a balloon density apparatus. Similar to the moisture content profiles, readings were taken at 0.9 meter increments beginning at the bottom of the pile of rock crushing fines and continuing to the top. The balloon density test procedure for measuring volume of a hole is found in ASTM D 2167.

The device is calibrated by making an initial reading on a level and smooth surface. The initial reading is obtained by placing the apparatus, shown in Figure 23, on the level surface and pumping the balloon down with the rubber bulb until the volume does not change. This reading is recorded. The bulb is then reversed and the balloon is pumped back into the cylinder.



Figure 23: Balloon density apparatus

In the field, the test site should be relatively planar. A small hole should be dug approximately four inches in diameter and 4 inches deep. All the soil removed from the hole should be retained in a sealed container to measure the mass and water content, to be used for density calculations. The balloon density apparatus is then placed over the hole and the balloon pumped into the hole until the volume is constant. Then a volume reading is taken.

To determine the density of the soil, the moisture content must be calculated using Equation 32 (ASTM D 2167):

$$w = \frac{\text{weight of water}}{\text{dry weight of soil}} \times 100 \quad (32)$$

The volume and wet and dry densities were calculated as shown in the following equations (ASTM D 2167):

$$V = V_2 - V_1 \quad (33)$$

$$\rho_w = \frac{W_w}{V} \quad (34)$$

$$\rho_D = \frac{\rho_w \times 100}{100 + w} \quad (35)$$

where,

V = volume of hole (cm³)

V_1 = initial volume reading (cm³)

V_2 = final volume reading (cm³)

ρ_w = wet density (g/cm³)

W_w = wet weight of soil (g)

ρ_D = dry density (g/cm³)

w = moisture content (%)

4. Results

4.1 Material Characterization

4.1.1 Slurry properties

A. Grain size distribution

The grain size distribution of the rock crushing fines was done using 0.595 mm (US no. 30), 0.297 mm (US no. 50), 0.149 mm (US no. 100), and 0.075 mm (US no. 200) sieves. The average percent passing is shown in Table 1:

Sieve Size (mm)	Avg. % Passing
0.595	97.7%
0.297	94.5%
0.149	69.8%
0.075	14.0%

Table 1: Average % passing

The percent passing values may be skewed towards the larger sizes because the soil particles clumped together. Therefore the particles had to be broken up to get a better analysis of the grain size distribution. As the sieve size decreased, it was harder to tell if the particles were clumped together or if they were broken up. Figure 24 shows a chart of the grain size distribution tests done by mechanical shaking. The graph shows a fairly uniform grading with particle sizes predominately between 0.07 mm and 0.3 mm. The uniformity coefficient, C_u , was 1.986, as calculated in Equation 36. A uniform soil has C_u values less than 5.

$$C_u = \frac{D_{60}}{D_{10}} = \frac{0.145}{0.073} = 1.986 \quad (36)$$

The coefficient of curvature, C_z , was 0.715, calculated in Equation 37. A well graded soil has a C_z value between 1 and 3 with a C_u value greater than 6. Both C_z and C_u were calculated using the average of the three curves. The curves were very close which indicates a very uniform soil.

$$C_z = \frac{(D_{30})^2}{D_{10} \times D_{60}} = \frac{(0.087)^2}{0.073 \times 0.145} = 0.715 \quad (37)$$

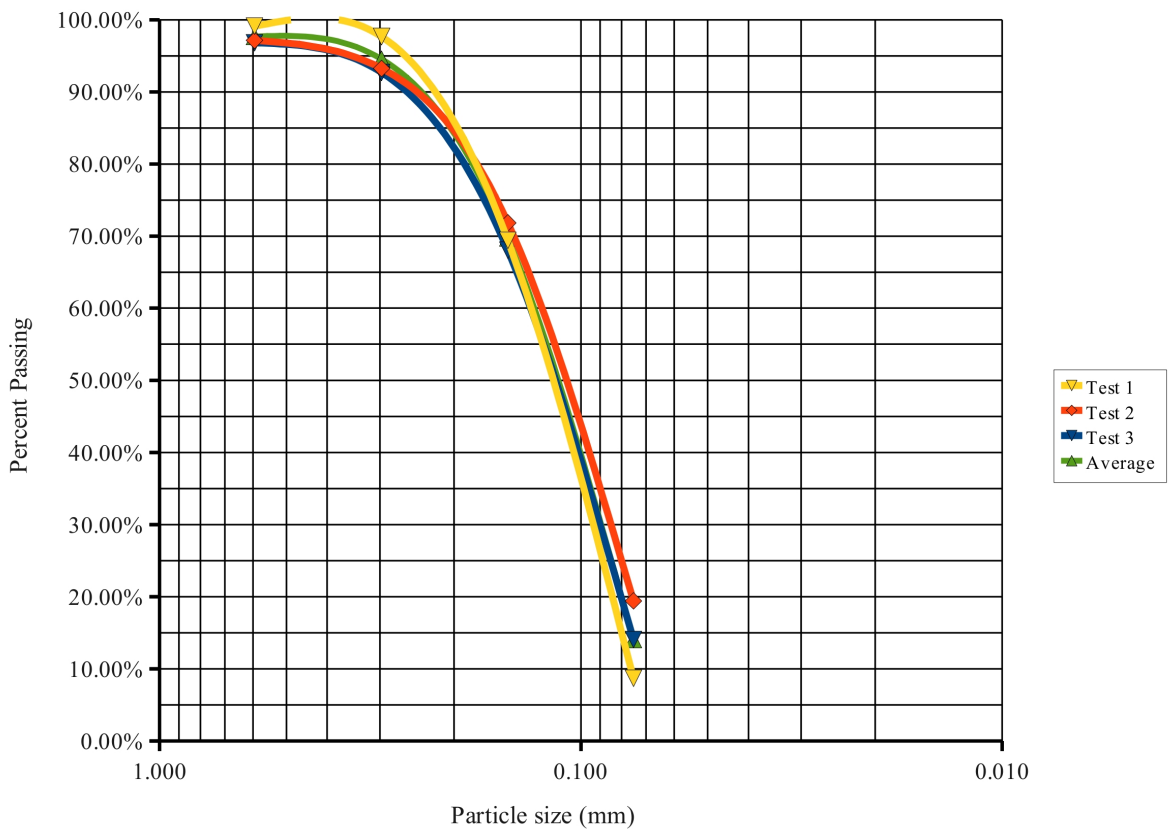


Figure 24: Rock crushing fines grain size distributions

B. Air Jet testing for grain size distribution

Air Jet testing was used to estimate the gradation of particles passing the 0.075 mm sieve.

The Air Jet test blows air to circulate the particles and has a vacuum to draw the particles through

the sieve to allow measurement of the smaller particles. This was useful because the smallest sieve size used for mechanical shaking GSD was a 0.075 mm sieve. Table 2 shows the average percent of particles passing each sieve size.

Sieve Size (mm)	Avg % Passing
0.210	99
0.150	81.08
0.075	42.39
0.038	18.65
0.020	7.12

Table 2: Average Air Jet grain size distribution

Figure 25 shows that the grain size distribution of the Air Jet sieving was also uniform. The particles are mostly the same size. The uniformity coefficient, C_u , was 4.689. The coefficient of curvature, C_z , was 1.111.

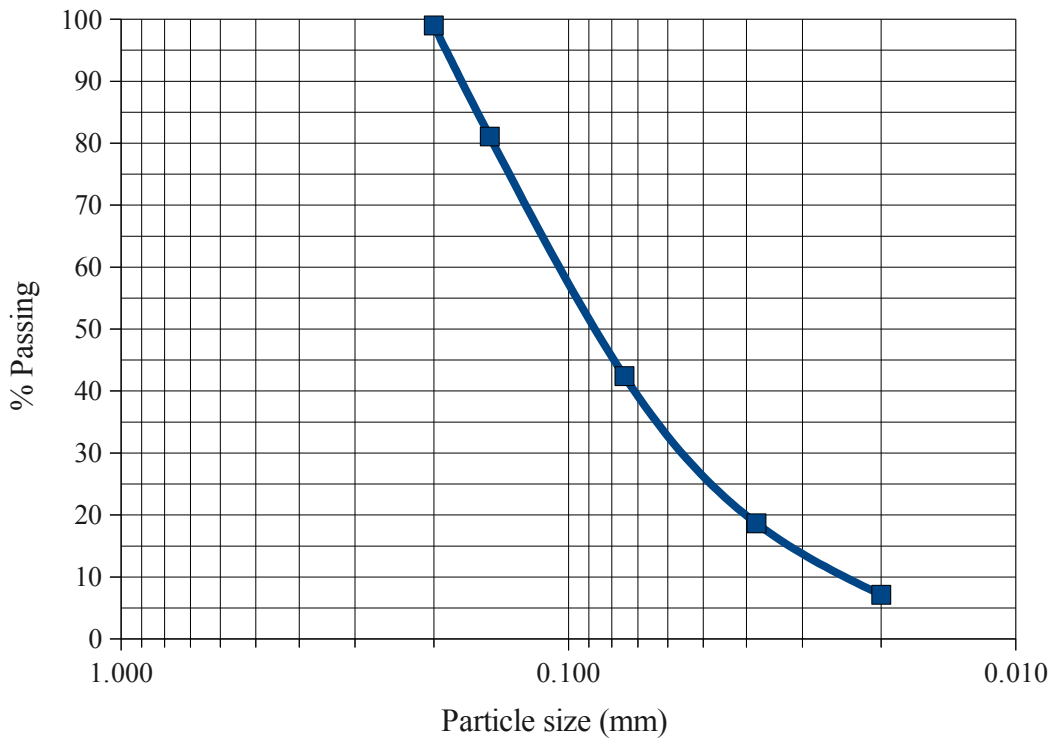


Figure 25: Air Jet grain size distribution

C. Specific gravity of solid particles

Specific gravity is the ratio of the weight of a given volume of aggregate to the weight of an equal volume of water (ASTM D 854). The specific gravity tests were run twice, the runs were compared and the results averaged. The two runs differed less than 0.5% which was acceptable error according to ASTM D 854. The results of the specific gravity test are in Table 3.

Specific Gravity	Test 1	Test 2	error (%)	Avg
Bulk SSD	2.68	2.67	0.37	2.68
Bulk	2.62	2.61	0.50	2.62
Apparent	2.79	2.78	0.18	2.78

Table 3: Specific gravity of rock crushing fines

The bulk saturated surface dry (SSD) specific gravity was 2.68 and is the ratio of the weight of a sample, including water in the void spaces, to an equal volume of water. The bulk specific gravity was 2.62 and is the ratio of the weight in air of the dry solids to that of an equal volume of water. The apparent specific gravity was 2.78. Apparent specific gravity is a ratio of the weight of the solid portion of the particles, not including the pores, to the weight of an equal volume of water. The material mined from the Barin quarry was granite and a bulk SSD of 2.68 is very close to the value given by Vulcan Materials of 2.7 (Vulcan Materials, 2009). Bulk SSD is most commonly used when considering aggregate for portland cement concrete. Bulk and apparent specific gravity are more commonly used in asphalt mixtures (Georgia Tech, 2009). The rock crushing fines would be saturated during the RDT and HBT. Therefore, the bulk SSD value of 2.68 was used in calculations requiring specific gravity because it accounted for the volume of the pores inside the rock crushing fines.

D. Particle angularity

Particle angularity affects the drainage characteristics of a material because angular particles do not compact as readily as rounded particles because their angular surfaces tend to lock up with one another and resist compaction, while smoother, more rounded surfaces tend to pass by one another allowing for easier compaction (Pavement Interactive, 2009). Increased void content indicates greater angularity, less sphericity, or rougher surface texture, or combination thereof (ASTM C 1252). Therefore, the higher the measured uncompacted void content, the more angular the material. The average uncompacted void content for the rock crushing fines was 58.7% with a specific gravity of 2.68. Because of the harsh abrasion that occurs when rocks are crushed, the rock crushing fines were expected to be highly angular. The uncompacted void content only gives an estimation of the angularity of particles in relation to other fine aggregates. Because only one aggregate was tested, pictures of the rock crushing fines particles were taken to visually assess the angularity of the particles. Figure 26 shows the crushed rock particles at 400x magnification. The angularity is clearly visible, as expected for crushed rock.

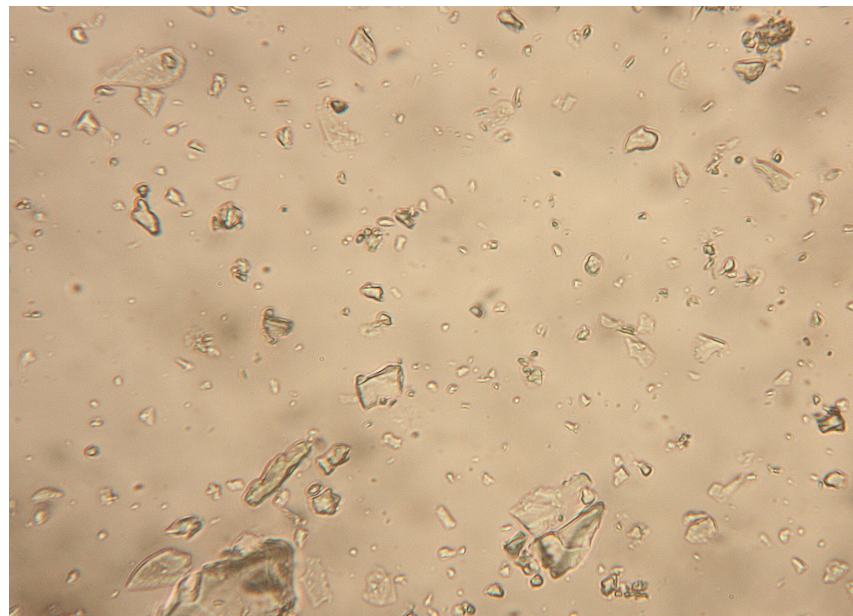


Figure 26: Crushed rock particles at 400x magnification

E. Atterberg Limits

The Atterberg limits provide basic information about soil used to estimate strength and settlement characteristics (University of Maine, 2009). The plastic limit test was attempted but the soil thread would break before the desired diameter of 3.2 mm was reached. The liquid limit is defined by ASTM D 4318 as the water content at which it takes 25 blows to close the gap when using the liquid limit device. Three liquid limit tests were conducted and the results graphed to determine the liquid limit of the rock crushing fines. To determine the liquid limit, which is a boundary between the liquid and plastic states, the three tests were conducted at different water contents so as to achieve different numbers of blows. The water content and number of blows for each test are in Table 4:

Water Content	# Blows
Test 1	
25.7%	21
Test 2	
29.9%	30
Test 3	
26.5%	27

Table 4: Water content and number of blows for liquid limit tests

The data from the three tests were plotted with the number of blows versus the water content on a semi-logarithmic plot, shown in Figure 27. From Figure 27, the liquid limit was 27.08%. The liquid limit was due to apparent cohesion caused by the surface tension of the water surrounding the particles. This is evident when conducting plastic limit tests because rolling the soil into a thread causes it to crumble, which is typical for soils exhibiting apparent cohesion.

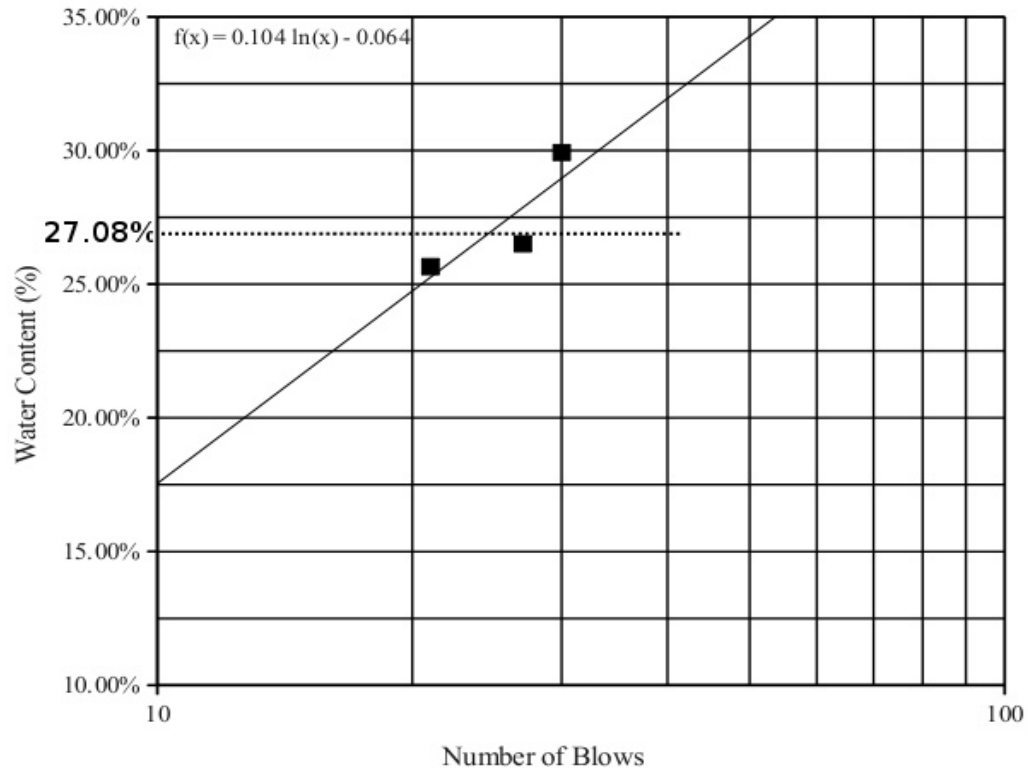


Figure 27: Liquid limit test

Dilatancy tests were also conducted on the rock crushing fines. Dilatancy is the observed tendency of a compacted granular material to dilate as it is sheared (ASTM D 2488). The dilatancy test is a quick test used for visual classification of the soil regulated by ASTM D 2488, the Standard Practice for Description and Identification of Soils (Visual – Manual Procedure).

Small sample of moist soil was placed in the palm of a hand. If the sample was lightly vibrated, the soil densified and water quickly appeared on the surface. Squeezing the sample caused a volume increase due to the shear stresses and the water disappeared from the surface.

4.1.2 Geotextile properties

A. Apparent Opening Size (AOS)

The AOS for each geotextile was not measured as part of this research. Rather, the values

given by the geotextile manufacturers were used. Table 5 lists the geotextiles and the AOS values given by the manufacturer.

	Geotextile	AOS, mm (US sieve no.)
1	Belton Industries Style 1853 4x6	0.355 (45)
2	Huesker Comtrac 175.175 DW	0.270 (50)
3	Propex Geotex 4x6	0.425 (40)
4	TenCate GT 500	0.425 (40)
5	Maccaferri Mactube MTOS400	0.425 (40)
6	Tensar Triton Tube TT712	0.068 (230)
7	Tensar Triton Tube TT716	0.976 (18)

Table 5: Geotextile AOS comparison

Geotextiles one through five had a similar AOS, shown in Table 5. The geotextile tubes from Tensar, the TT712 and TT716, had an AOS of 0.068 mm and 0.976 mm respectively and were the only two that varied greatly from the mode. Geotextiles one through five were expected to perform similarly during the HBT and geotextiles six and seven were expected to have different results from the others. However, all geotextiles had similar results as shown in Section 4.2.4.

B. Bubble Point Test

The bubble point test (BPT) was used to characterize the pore size distribution of the geotextiles and compare all of the geotextiles tested. Figure 28 shows the BPT results for all the geotextiles. The pore distribution for the six geotextiles tested was predominately well-graded. A geotextile with a well-graded distribution, or wide range of sizes, has a uniformity coefficient (C_u) greater than 10.

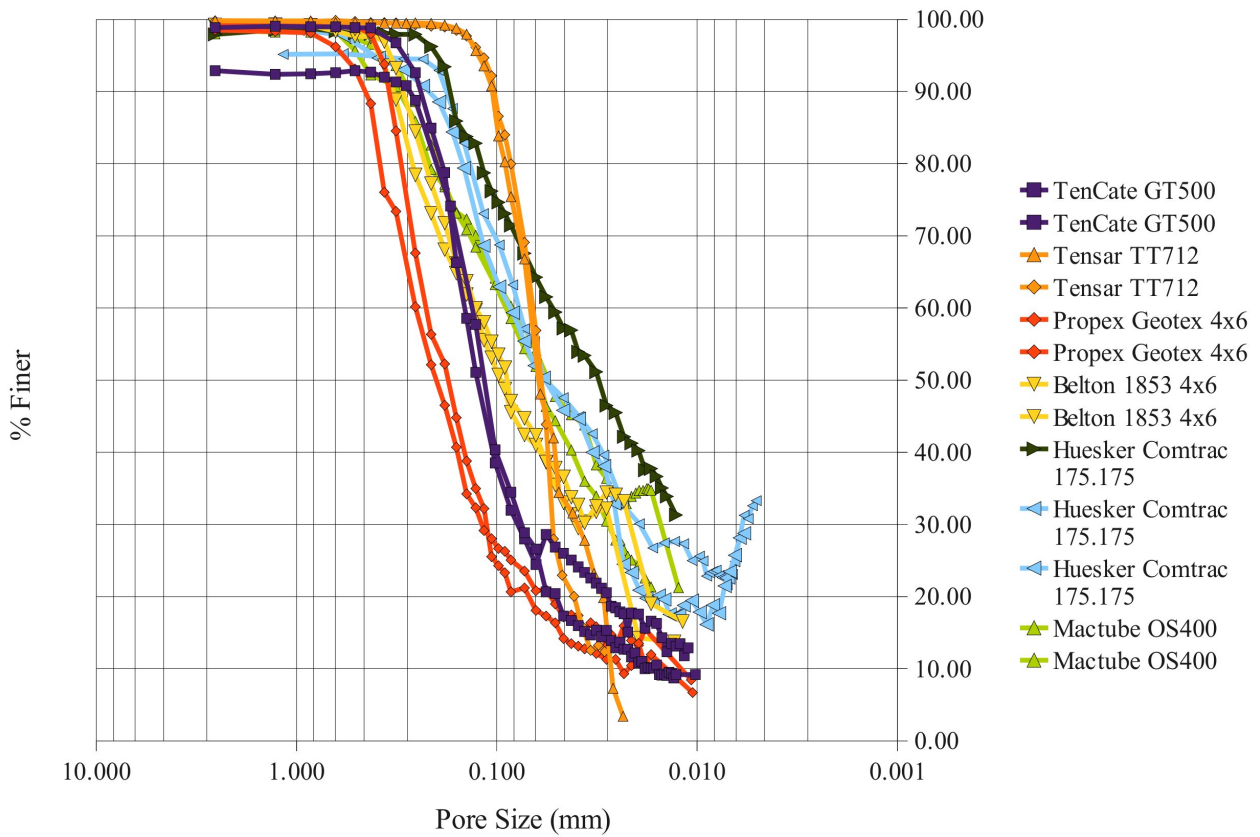


Figure 28: Bubble point test results

The Tensar TT712 and TenCate GT500 are the exceptions, with a C_u of 2.48 and 8.13 respectively. A C_u less than 5 indicates uniform distribution. The average uniformity coefficient for each geotextile can be seen in Table 6.

Geotextile	C_u
Tencate GT500	8.13
Tensar TT712	2.48
Propex Geotex 4x6	15.94
Belton 1853	21.25
Huesker Comtrac 175.175 DW	16.66
Mactube OS400	13.93

Table 6: Uniformity coefficient from BPT

C. Wide width strength test

The wide width strength test, ASTM D 4595, was not conducted as part of this research program as the manufacturer's values were considered adequate. The manufacturer's values for wide width strength in both the machine direction (MD) and cross machine direction (XD) are in Table 7. Machine direction is the direction parallel to the direction of fabric movement during the manufacturing process and cross machine direction is perpendicular to the movement during the manufacturing process. A higher value indicates greater strength.

Wide width strength test is useful during the design of a geotextile tube because it indicates the forces that the geotextile can withstand.

Geotextile	Wide Width Strength MD (kN/m)	Wide Width Strength XD (kN/m)
Belton Industries Style 1853 4x6	70	105
Huesker Comtrac 175.175 DW	175	175
Propex Geotex 4x6	70	105
TenCate GT 500	70	96
Maccaferri Mactube MTOS400	70	101
Tensar Triton Tube TT712	121	121
Tensar Triton Tube TT716	158	201

Table 7: Wide width strength test comparison, ASTM D 4595

D. Seam Strength

The seam strength was not tested as part of the research program, therefore, the manufacturer's data was used. Table 8 lists the manufacturer's values, if provided, for seam strength calculated using ASTM D 4884. Seam strength is important when designing geotextile tubes to ensure that the seams do not rupture during use.

Geotextile	Seam Strength (kN/m)
Belton Industries Style 1853 4x6	NA
Huesker Comtrac 175.175 DW	NA
Propex Geotex 4x6	NA
TenCate GT 500	70
Maccaferri Mactube MTOS400	70
Tensar Triton Tube TT712	70
Tensar Triton Tube TT716	140

Table 8: Seam strength comparison, ASTM D 4884

E. Water flow rate (permeability)

The water flow rate values were obtained from the manufacturers. The values were not calculated as part of this research program. Table 9 gives the water flow rate values given by the manufacturers as per ASTM D 4491.

Geotextile	Water Flow Rate (L/min/m²)
Belton Industries Style 1853 4x6	7.03
Huesker Comtrac 175.175 DW	8.44
Propex Geotex 4x6	7.03
TenCate GT 500	7.03
Maccaferri Mactube MTOS400	9.67
Tensar Triton Tube TT712	27.43
Tensar Triton Tube TT716	59.42

Table 9: Water flow rate comparison, ASTM D 4491

F. Ultraviolet Resistance

The values for ultraviolet resistance, calculated using ASTM D 4355, were provided by the manufacturers and were not found as part of this research program. Table 10 lists the ultraviolet resistance of the geotextiles tested.

Geotextile	Ultraviolet Resistance (%)
Belton Industries Style 1853 4x6	70
Huesker Comtrac 175.175 DW	NA
Propex Geotex 4x6	80
TenCate GT 500	80
Maccaferri Mactube MTOS400	80
Tensar Triton Tube TT712	59
Tensar Triton Tube TT716	59

Table 10: Ultraviolet resistance comparison, ASTM D 4355

4.1.3 Effect of Polymers

The six main polymers tested as part of this research program are listed in Table 11. Each polymer was used with the rapid dewatering test at several different concentrations of 0.3, 0.03, 0.006, 0.003, and 0.0015% of the slurry weight. A full chemical breakdown of the polymers can be seen in the appendix.

Solve # 153
Solve # 154
Solve # 163
Solve # 2250A
Solve # 9310
Solve # 9350

Table 11: Polymers tested using RDT

After running rapid dewatering tests (RDT) with the polymer concentrations listed above, 0.006% by weight of the slurry proved to be the most effective at increasing the dewatering efficiency.

Figure 29 shows the concentration of Solve # 9310 at varying concentrations.

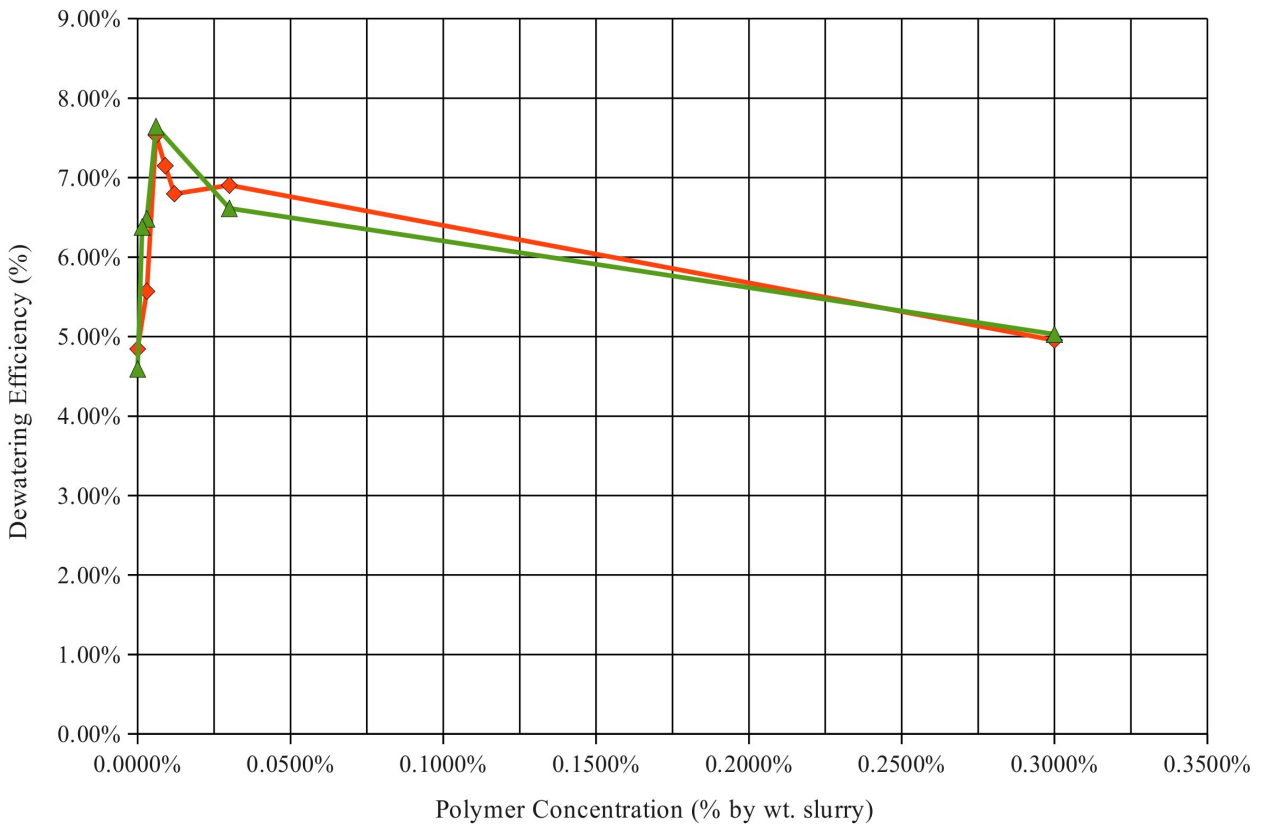


Figure 29: Dewatering efficiency of Solve 9310 at varying concentrations

Once the ideal concentration was determined, the RDT was run with the six polymers listed above at a concentration of 0.006% by weight of the slurry and compared with one another. As shown in Figure 30, the percent dewatering, which is the difference between the initial and final water contents, ranged from 17.1% to 25.8%. This was not a large difference in performance, and previous tests showed that initial water content caused a greater percent dewatering. Therefore, the polymer Solve # 9310 was chosen for testing during the hanging bag test because it had the highest percent dewatering at the lowest initial water content.

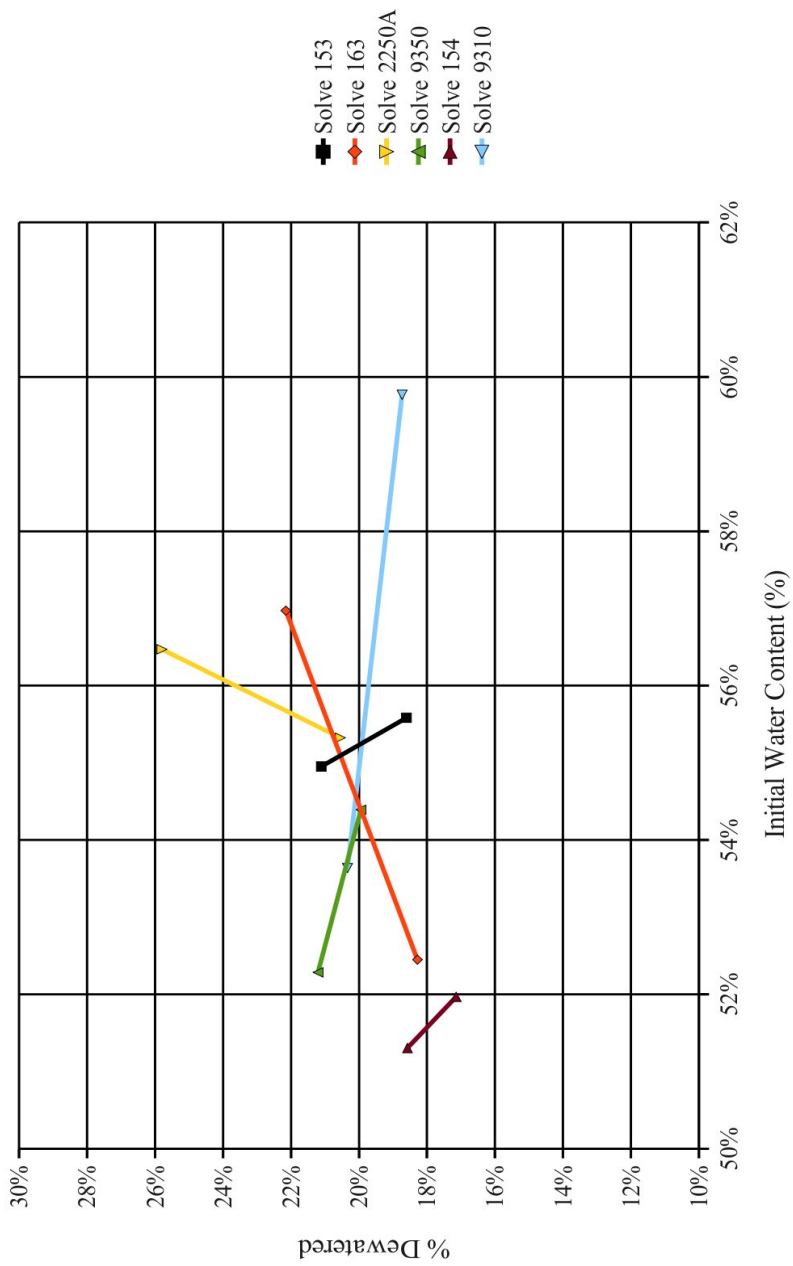


Figure 30: Comparison of Polymer Dewatering Efficiency at 0.006% Concentration

4.2 Laboratory Studies

4.2.1 Consolidation

Consolidation tests were run in order to determine how the rock crushing fines would consolidate. The information will provide an indication of what happens during the dewatering process as the fines consolidate due to drainage and overburden pressure. A Levermatic Consolidation Apparatus was used to perform the tests. Figure 31 shows the results.

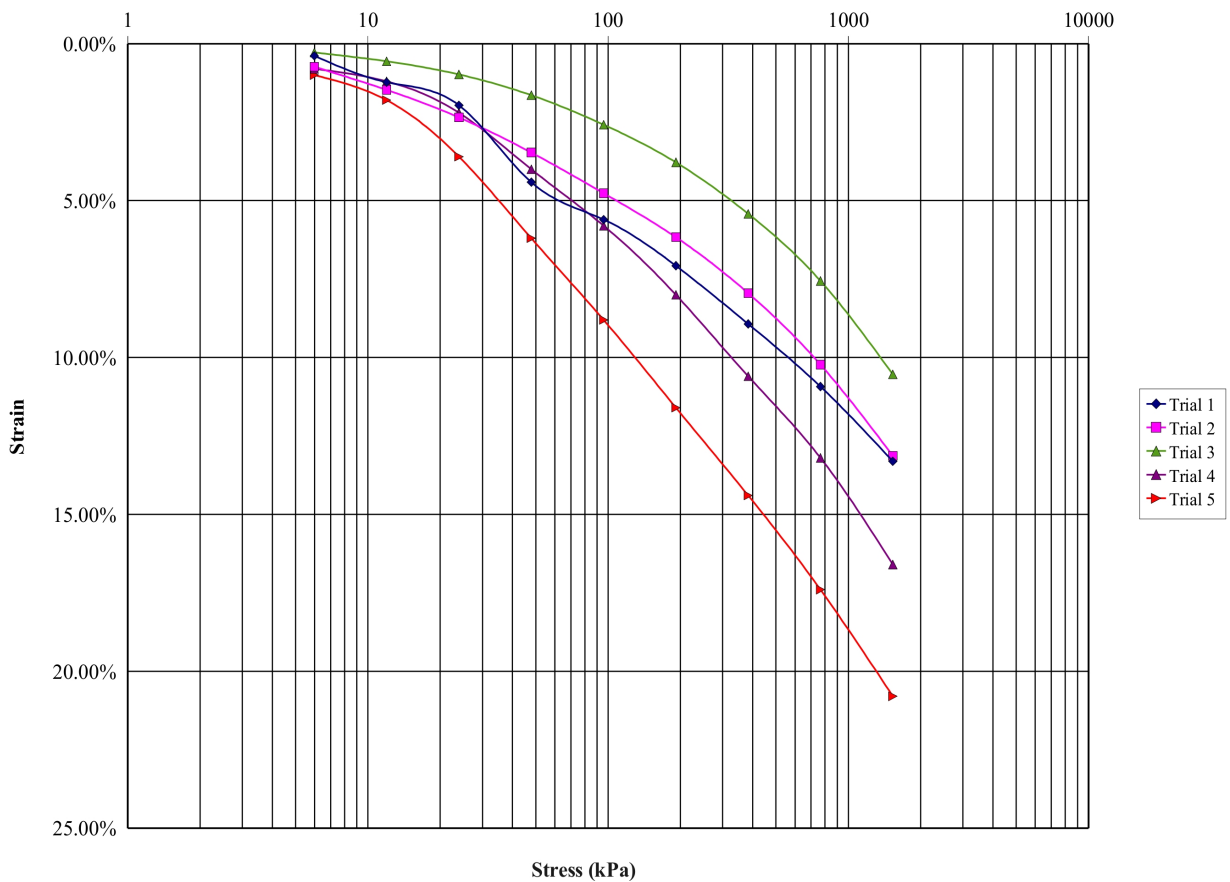


Figure 31: Consolidation strain vs log stress

Each point on the graph is double the stress of the previous point. There was no secondary consolidation observed. The increase in strain was larger with each incremental stress. The

compression index, C_c , was calculated for each trial using Equation 38.

$$c_c = \frac{\Delta e}{\Delta \log \sigma'_v} \quad (38)$$

where,

C_c = compression index

e = void ratio

σ'_v = imposed test pressure (kPa)

Table 12 shows the compression index for each trial. C_c is an indicator of compressibility (Gregory, et al, 2006). Table 12 shows the values of C_c for each trial in Figure 29.

Trial	C_c
1	0.064
2	0.070
3	0.066
4	0.090
5	0.100
Mean	0.08
Standard Deviation	0.02

Table 12: Compression index

Figure 32 shows the dial reading in inches vs time in seconds. The stress was 5.99 kPa. The stress was applied at 10 seconds and caused a rapid settlement. The consolidation of the sample, due to the applied stress, slowed after 15 seconds. The coefficient of consolidation was calculated with Equation 39. The data for the other stress increments is in Appendix 1.

$$c_v = \frac{(T_v) \left(\frac{H_{avg}}{2} \right)^2}{t_{50}} \quad (39)$$

where,

c_v = coefficient of consolidation (in²/min)

T_v = time factor for 50% consolidation

H_{avg} = average sample thickness for the range of loading considered (in)

t_{50} = time for 50% consolidation to occur (min)

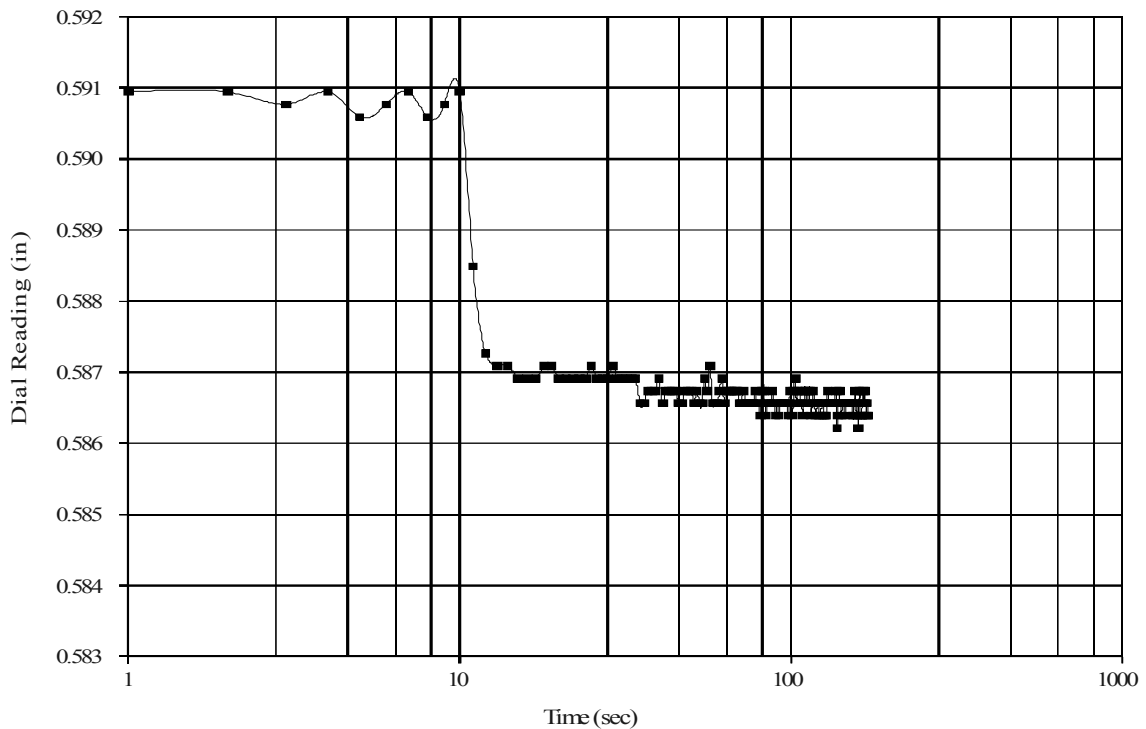


Figure 32: Consolidation dial reading vs time for 5.99 kPa of applied stress

Table 13 shows the coefficient of consolidation, c_v , calculated for each stress applied to the sample.

The coefficient of consolidation is the factor governing the rate at which compression can occur.

The rate and amount of compression varies with the rate at which pore water pressure is lost

(Allaby, A. and Allaby, M., 2009). As c_v increases, the rate of compression increases. The consolidation graphs in Appendix 1 show that the largest settlements were seen in correlation with the higher coefficients of consolidation.

Stress (kPa)	c_v (cm ² /min)
5.99	0.613
11.97	0.471
23.94	0.594
47.88	3.174
95.76	3.071
191.52	1.716
383.04	1.297
766.08	1.606
1532.16	1.800
Average	1.594

Table 13: Coefficient of consolidation for each stress increment

Two Air Jet tests were conducted on the rock crushing fines after the consolidation tests to evaluate if grain crushing occurred. Table 14 shows the results from the Air Jet tests compared to the original Air Jet tests not subjected to consolidation testing.

Sieve Size, US (µm)	Average Percent Passing	
	Before Consolidation	After Consolidation
100 (150)	81.1%	88.6%
200 (75)	42.4%	59.8%
400 (38)	18.7%	33.2%
635 (20)	7.1%	14.8%

Table 14: Air Jet Test Comparison Before and After Consolidation

The average percent passing the 75, 38, and 20 µm sieves after consolidation were larger than the average percent passing those sieve before consolidation. This indicates grain crushing.

4.2.2 Permeability

Permeability testing was conducted using a constant head permeability test. The constant head test was used because the rock crushing fines are granular. The constant head test apparatus is shown in Figure 33.



Figure 33: Constant head permeability Test

The permeability was calculated as described in Section 3.4.2. The coefficient of permeability (k) and density (ρ) for the tests are shown in Table 15. The average k value was 1.52×10^{-4} cm/s. This is within the typical values of 1×10^{-3} to 1×10^{-5} cm/s for rock crushing fines or silt proposed by Sehgal in 1967 (Venkatramaiah, 2006).

Test	k (cm/s)	ρ (g/cm ³)
1	2.36E-4	1.16
2	2.41E-4	1.18
3	2.97E-4	1.14
4	5.48E-5	1.30
5	1.22E-5	1.50
6	6.82E-5	1.47
Avg	1.52E-4	

Table 15: Results of permeability testing

Figure 34 shows a plot of permeability versus density. As density increases, permeability decreases. The rate of decrease is very small as indicated by the equation of the straight line showing the slope is equal to -0.001.

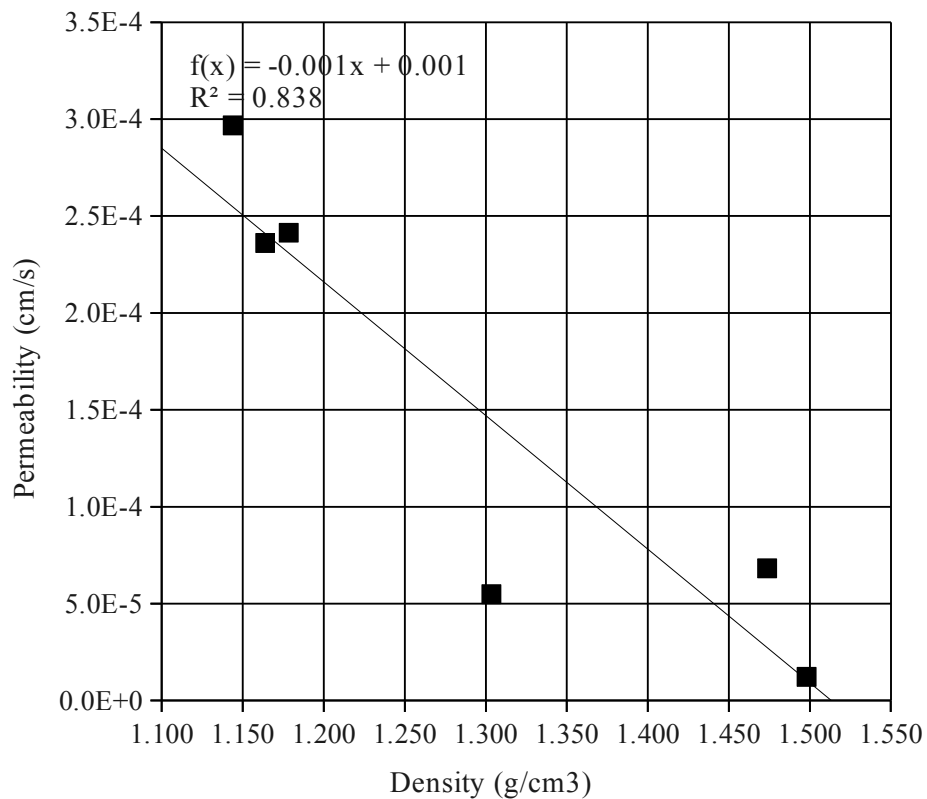


Figure 34: Permeability vs Density results of permeability tests.

4.2.3 Rapid Dewatering Test (RDT)

A. Without polymer

The rapid dewatering test (RDT) was conducted without polymer to test the dewatering efficiency of the geotextiles. Table 16 shows the results of the RDT without polymer. The average percent dewatered was 25.8%.

Geotextile	Initial Water Content	% Dewatered
GT 500 (Tencate)	53.7%	44.0
GT 500 (Tencate)	46.2%	24.8
GT 500 (Tencate)	43.9%	24.9
GT 500 (Tencate)	46.3%	19.9
GT 500 (Tencate)	55.0%	20.0
GT 500 (Tencate)	68.0%	32.4
TG 500 (Evergreen)	46.6%	22.3
TG 500 (Evergreen)	46.9%	18.4
Avg % Dewatered		25.8

Table 16: RDT without polymer

An increase in initial water content resulted in higher percent dewatered as shown in Figure 35. The outlier with an initial water content of 53% was attributed to operator error and was not included in the calculation of the trendline. The variations were attributed to user error in bumping the table while the test was in progress, causing an increased flow for a short period of time.

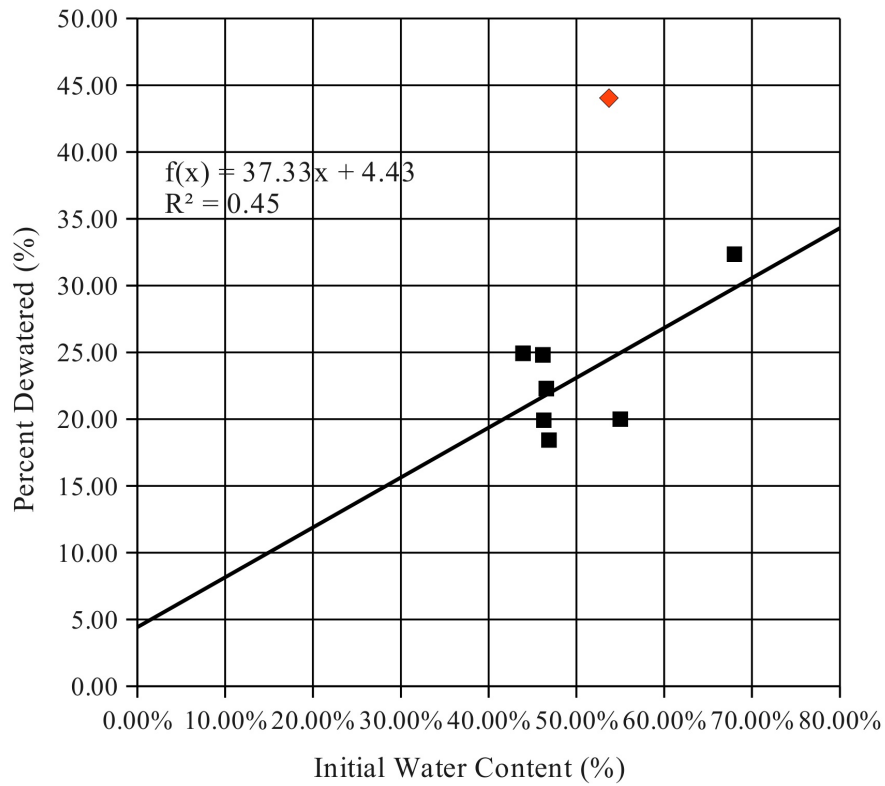


Figure 35: Percent dewatered vs Initial water content from RDT without polymer

B. With Polymer

The results of the RDT with polymer are shown in Table 17. All tests were done using TenCate's GT500 geotextile. The percent dewatered is the difference between initial and final water contents. The percent dewatered ranged from a low of 17.1% to a high of 25.8%. The average percent dewatered was 20.2%.

Date:	05/20/09	05/21/09	05/20/09	05/21/09	05/20/09	05/21/09
Polymer	Solve 153	Solve 153	Solve 163	Solve 163	Solve 2250A	Solve 2250A
% Polymer by Weight of Slurry	0.006%	0.006%	0.006%	0.006%	0.006%	0.006%
Initial Water Content	55.6%	55.0%	57.0%	52.4%	55.3%	56.5%
Final Water Content	45.2%	43.4%	44.3%	42.9%	44.0%	41.9%
% Dewatered	18.6%	21.1%	22.2%	18.3%	20.5%	25.8%

Date:	05/20/09	05/21/09	05/20/09	05/21/09	04/14/09	04/30/09
Polymer	Solve 9350	Solve 9350	Solve 154	Solve 154	Solve 9310	9310
% Polymer by Weight of Slurry	0.006%	0.006%	0.006%	0.006%	0.006%	0.006%
Initial Water Content	54.4%	52.3%	52.0%	51.3%	53.6%	59.8%
Final Water Content	43.5%	41.2%	43.1%	41.8%	42.7%	48.6%
% Dewatered	19.9%	21.2%	17.1%	18.6%	20.3%	18.7%
Avg % Dewatered	20.2%					

Table 17: RDT with polymer

Considering the variance in initial water contents, the percent dewatered for the different polymers was considered to be negligible. The average percent dewatered of all tests using polymers was 20.2%, but the average percent dewatered for tests without polymer was 25.8%. Therefore, the polymers retained water and decreased the dewatering efficiency. The percent dewatered was primarily controlled by the initial water content, as shown in Figure 36.

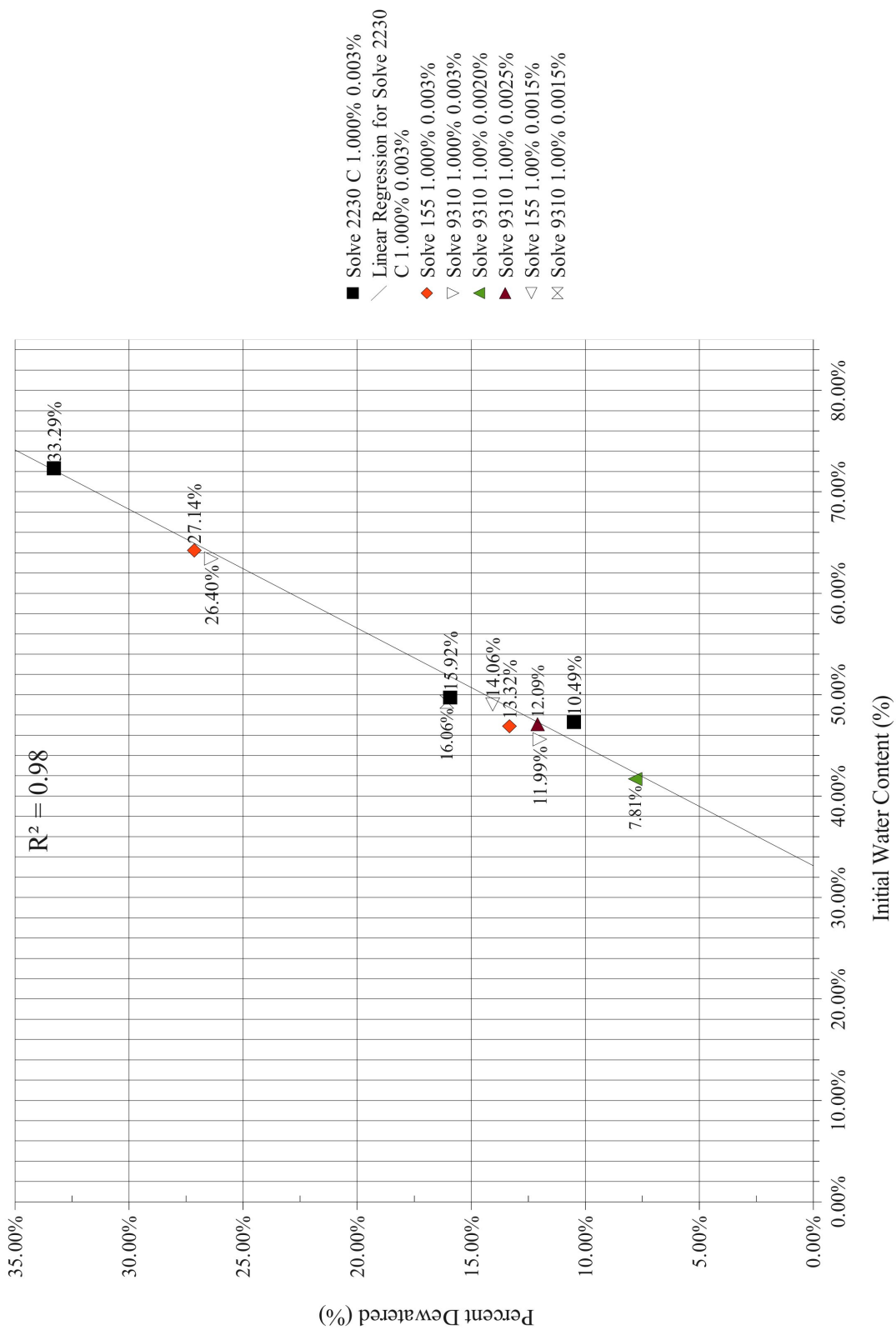


Figure 36: Percent dewatered vs Initial water content with polymer

4.2.4 Hanging Bag Test (HBT)

A. Without polymer

Table 18 shows the results of the hanging bag tests conducted without polymer. It was expected that the tests with a higher initial water content would have a slightly lower 24 hour water content. This hypothesis held true, as shown in Figure 34. The filter cake on the geotextile allows the geotextile to filter the rock crushing fines. Piping, particles passing through the geotextile, occurred initially, but quickly began to slow. The amount of particles passing through the geotextile decreased significantly during the first 30 minutes of the test, as long as the hanging bag was not agitated. Agitation caused more particles to pass through the geotextile because the filter cake was disturbed.

Date	06/30/09	07/14/09	09/01/09	09/24/09
Fabric	Tencate GT 500	Propex Geotex 4 x 6	Tensar TT 712	Mactube OS400
Polymer	NA	NA	NA	NA
Initial Water Content	52%	49%	51%	50%
24 hr Water Content	28%	34%	28%	28%
Removal Efficiency	99.8%	99.3%	99.8%	99.7%
Weather at start of test	Sunny, 90F 30% Humidity	Cloudy, 72F 85% Humidity	Cloudy, 72F 85% Humidity	Cloudy, 73F 85% Humidity

Date	07/21/09	07/29/09	09/15/09	09/29/09
Fabric	Comtrac 175.175 DW	Belton 1853	Tensar TT 716	Mactube OS400
Polymer	NA	NA	NA	NA
Initial Water Content	49%	51%	49%	48%
24 hr Water Content	34%	31%	29%	29%
Removal Efficiency	99.5%	99.0%	99.4%	99.3%
Weather at start of test	Sunny, 84F 40% Humidity	Rainy, 74F 90% Humidity	Cloudy, 78F 93% Humidity	Cloudy, 75F 83% Humidity

Table 18: Results of HBT without polymer

B. With polymer

Solve 9310 was the polymer used for the HBT. As shown in Section 4.2.3, there was not a

polymer that outperformed the others, therefore, Solve 9310 was chosen as it provided the highest percent dewatering at the lowest initial water content. Table 19 shows the HBT results with Solve 9310 polymer added. The Huesker Comtrac 175.175 DW was the only geotextile that had a lower 24 hour water content when using Solve 9310. The 24 hour water content was 32% with Solve 9310 and 34% without. This could be attributed to a higher initial water content in the test with polymer.

Date	07/07/09	07/09/09
Fabric	Tencate GT 500	Propex Geotex 4 x 6
Polymer	Solve 9310	Solve 9310
Initial Water Content	49%	47%
24 hr Water Content	30%	34%
Removal Efficiency	99.8%	99.7%
Weather at start of test	Cloudy, 79F 80% Humidity	Cloudy, 73F 83% Humidity

Date	07/23/09	07/27/09
Fabric	Comtrac 175.175 DW	Belton 1853
Polymer	Solve 9310	Solve 9310
Initial Water Content	50%	51%
24 hr Water Content	32%	34%
Removal Efficiency	99.7%	99.5%
Weather at start of test	Sunny, 73F 88% Humidity	Partly Cloudy, 86F 64% Humidity

Table 19: Results of HBT with polymer

4.3 Field Studies

The results of the in situ tests conducted at Barin Quarry are below.

4.3.1 Moisture Content Profiles with Moisture Probe

A. Calibration

The Fieldscout TDR 300 moisture probe was tested prior to use at Barin Quarry to determine if a new calibration for the in situ soil was needed or if the provided volumetric water content

(VWC) calibration would work. Table 20 shows the results for the calibration testing. The values obtained during the calibration testing showed that the standard VWC calibration already on the Fieldscout would be sufficient and no further calibration was needed. The Fieldscout was more accurate at higher water contents.

Target w (%)	Water Content	TDR VWC (%)
5	5.24%	2.90%
10	11.13%	8.60%
15	14.65%	15.00%
20	18.87%	20.30%
25	23.43%	26.00%
30	33.24%	33.70%
35	36.36%	34.00%
40	39.59%	41.10%
45	43.09%	42.50%

Table 20: Calibration testing for the Field Scout TDR 300

Figure 37 shows the relationship between the calculated water content and the Fieldscout TDR 300 VWC.

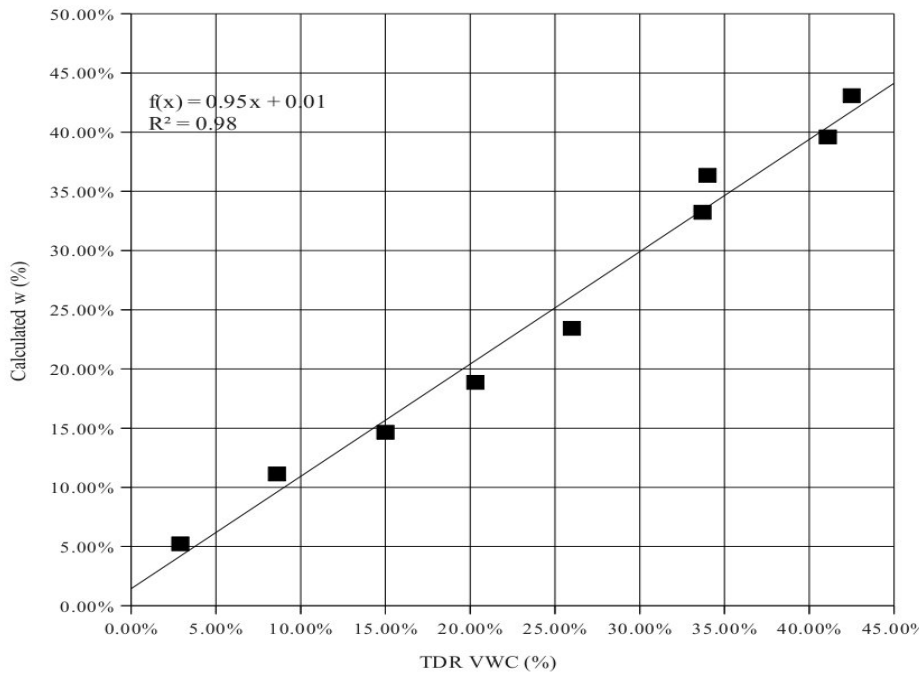


Figure 37: Calculated water content vs Field Scout VWC

The line in Figure 37 has an R^2 value of 0.98. The trendline shows that the water content value obtained by weighing a wet soil sample and comparing it to the dry weight of the same sample is very close to the values obtained using the Field Scout TDR 300 with the standard VWC measurement.

B. Field moisture profiles

Vertical in situ moisture content profiles of the rock crushing fines were taken at Barin Quarry to better understand how the piles drained. It was expected that the piles would have a higher water content near the base and that water content would decrease as elevation increased. Figure 38 shows the water content profiles. Each point on the graph is an average of three readings taken at that spot.

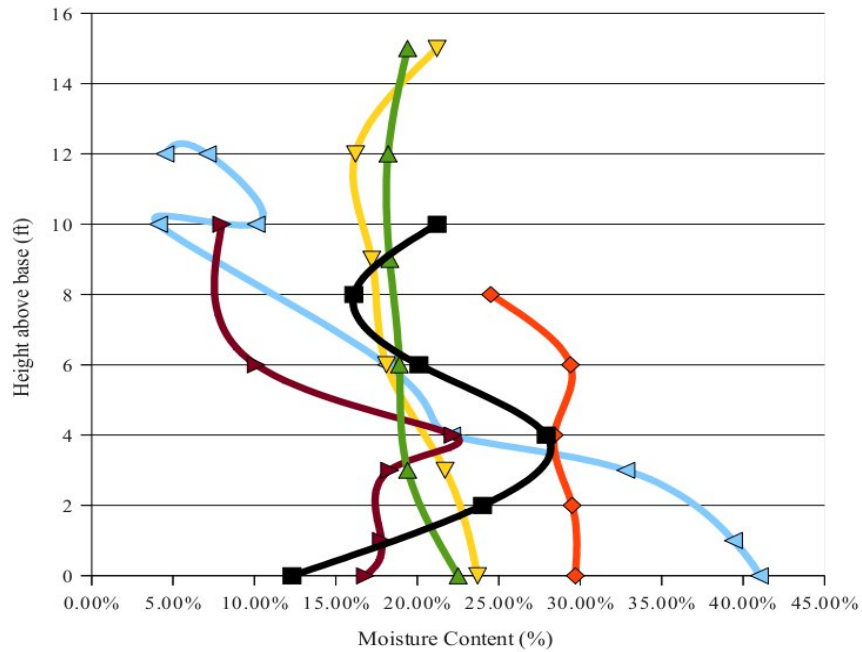


Figure 38: Moisture content profiles from Barin Quarry

There is a general trend of lower water contents closer to the top of the piles, but that was not

always true. The Fieldscout TDR 300 has a limited depth of measurement of 7.9 inches and therefore is only a measurement of surface water content. This may account for some variations that were seen between the different profiles. However, the primary differences can be attributed to local weather conditions, amount of rainfall, and the time the rock crushing fines sat in the sun.

4.3.2 Unit weight profiles

The unit weight profiles of the piles of rock crushing fines are shown in Figure 39. The average unit weight was 1.46 g/cm³. The unit weight values ranged from 1.07 g/cm³ to 1.80 g/cm³. There were two low values of 1.07 g/cm³ and 1.09 g/cm³, these were likely due to operator error. If the low values of 1.07 and 1.09 g/cm³ are thrown out, the average unit weight was 1.59 g/cm³.

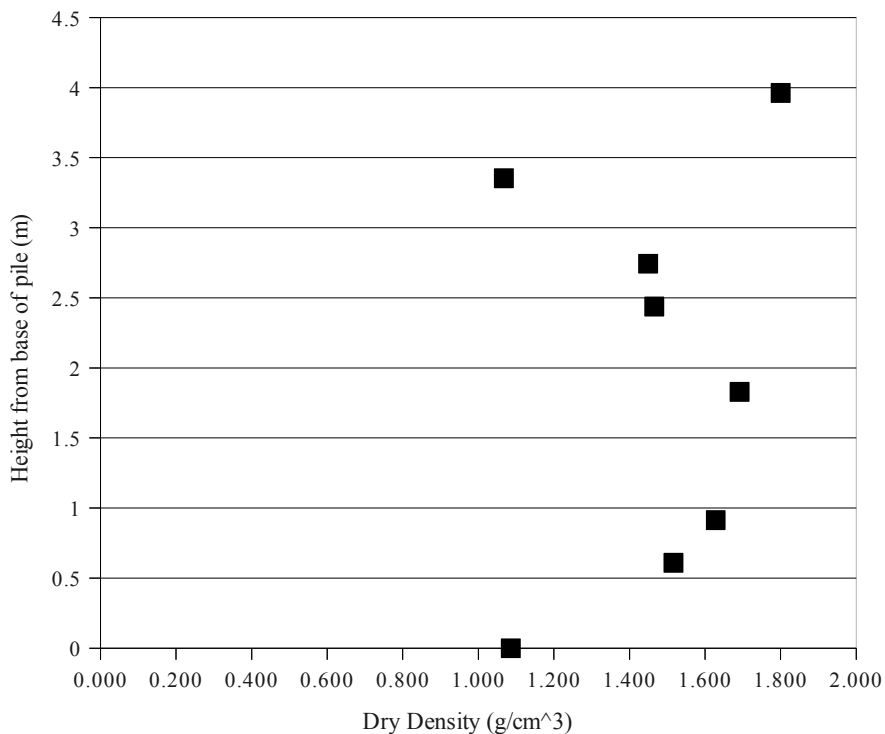


Figure 39: Unit weight profiles from Barin Quarry

5. Conclusions

The purpose of this paper was to study the efficiency of using geotextile tubes to dewater rock crushing fines. Rapid dewatering tests and hanging bag tests were conducted and the results were studied. Based on this study, the following conclusions were made.

5.1 Adequacy of RDT

The rapid dewatering test (RDT), developed by TenCate, was used to assess feasibility of using polymers to increase the dewatering efficiency of the geotextile tubes containing the rock crushing fines. The RDT is a useful tool to quickly analyze the dewatering efficiency of geotextiles and test the usefulness of polymers in the slurry. The RDT required ten minutes to complete and the results correlated well with the hanging bag tests, which required twenty four hours to complete. The RDT showed that the polymers impeded the dewatering process with these rock crushing fines, as was also seen with the HBT. The average percent dewatered for tests conducted without polymer was 25.8% and the average percent dewatered for tests conducted with polymer was 20.2%.

5.2 Adequacy of HBT

The hanging bag test (HBT) is a small scale test used to estimate field performance of full size geotextile tubes. The HBT allows analysis of the efficiency of a geotextile for dewatering a slurry. The HBT proved to be an effective laboratory test to determine the dewatering efficiencies of geotextiles as well as testing the usefulness of polymers in the slurry. Within twenty four hours the efficiency of a geotextile tube can be evaluated with a slurry sample of 115 liters. The HBT is

much cheaper to conduct than a full scale field test of geotextile tubes. The HBT conducted with the TenCate GT 500 material correlated with the results of the RDT conducted with the same material. The percent dewatered of the TenCate GT 500 HBT conducted without polymer in the slurry was 47% while the test conducted with polymer in the slurry had a percent dewatered of 39%. The other geotextiles tested, with one exception, exhibited similar results, i.e. the percent dewatered of tests conducted without polymer was higher than those conducted with polymer. The Huesker Comtrac 175.175 DW was the only geotextile which exhibited a higher percent dewatered when polymer was added to the slurry. The percent dewatered for the Huesker tests conducted without polymer and those conducted with polymer were 30% and 36% respectively. For all the tests there was only a 6% difference between those conducted with polymer and those conducted without. This was considered to be negligible due to the low number of tests conducted and the accuracy of the measurements taken.

5.3 Effect of geotextile on filtration

All seven geotextiles effectively filtered the rock crushing fines in the HBT. The average removal efficiency of all the HBT conducted was 99.6%. The removal efficiency is a ratio indicating the percent solids retained in the geotextile tube. The laboratory tests showed that all the geotextiles performed similarly and that conventional parameters for predicting geotextile filtration performance did not predict the results seen in the tests. Even when conventional geotextile-soil retention criteria were not satisfied, a large portion of the fines were retained inside the tube due to the filter cake that formed on the inside of the geotextile. The filter cake dominated the filtration process, masking the effects of the geotextile.

5.4 Effect of polymer on filtration

All of the polymers tested with the RDT during this research project exhibited similar results. The dewatering efficiency usually decreased when a polymer was used and the removal efficiency usually improved slightly, as shown by Table 19 in Section 4.2.4. The average percent dewatered of HBT without polymer was 40% and HBT with polymer was 34%. The average removal efficiency for HBT without polymer was 99.5% and those with polymer were 99.7%. The slight increase in removal efficiency does not offset the decrease in dewatering efficiency nor the time associated with adding the polymers to the slurry. All the polymers used during this research performed similarly regardless of chemical composition of the polymer. The use of polymers is not recommended for dewatering these rock crushing fines without further research.

5.5 Water content variation in the field

Variations of the water content in piles of fines in the field were likely caused by local weather and length of time that the fines had been allowed to drain.

5.6 Field moisture gauge results

The Fieldscout TDR 300 moisture probe was a quick and accurate means of testing water contents in the field. However, the Fieldscout was limited in its usefulness by its shallow testing depth of 7.9 inches. Using a similar method with longer testing rods would provide more accurate results since it is felt that the surface of large volumes of material dry faster than the inside and are prone to more moisture content fluctuations due to weather.

5.7 Consolidation testing

Consolidation tests showed that consolidation occurred quickly for these silts, within 45 minutes for 0.5 inch lab samples. The consolidation test required 30-45 minutes to apply the stress in nine increments totaling 1532.16 kPa. Table 13 in Section 4.2.1 shows the coefficient of consolidation, c_v , ranged from a low of 0.47 cm²/min at an applied stress of 11.97 kPa to a high of 3.17 cm²/min at an applied stress of 47.88 kPa. The coefficient of consolidation decreased at stresses higher than 47.88 kPa. A higher coefficient of consolidation indicates consolidation occurred rapidly at that applied stress.

Air Jet sieve tests proved that grain crushing occurred (see Section 4.2.1). Grain crushing is not expected to occur at low stresses and the stresses in geotextile tubes are not expected to exceed 30 kPa (Shin and Oh, 2007). It is expected that a reduction in the soil permeability caused by grain crushing of the fines would increase the dewatering time. Because the primary settlement is due to the expulsion of water from the sample, the time necessary for water to be expelled from fines with low permeability will be greater than for fines with a high permeability. An increase in stress is expected to increase the amount of dewatering in geotextile tubes due to water being expelled by the consolidation of the rock crushing fines.

6. Further Research

6.1 Field testing

Full scale field testing is necessary to evaluate the economic feasibility of geotextile tubes compared to settling ponds. A comparison of the time rate of dewatering of settling ponds versus geotextile tubes needs to be done.

The economic feasibility of using geotextile tubes to dewater rock crushing fines instead of settling ponds should be determined before the tubes are implemented. The scale of testing done during this research project was not sufficient to assess the economic aspect of using geotextile tubes versus continuing to use settling ponds. Pumps are required to pump the rock crushing fines into the geotextile tubes, the geotextile tubes must be purchased and they can only be used once, the man hours necessary to set up geotextile tubes, set up and maintain the pumps required for filling, and disposal of the tubes as well as the rock crushing fines are all factors that contribute to the cost of using geotextile tubes and must be analyzed before geotextile tubes are deployed commercially.

6.2 More extensive polymer testing

A more extensive examination of polymers could be done. A chemical analysis of the rock crushing fines should be done to assist in choosing a polymer that would speed up the dewatering process and increase the filtration efficiency. The RDT would be useful in evaluating additional polymers. Further research could show whether polymers have a greater effect on the dewatering process with different geotextiles or if polymers cause the same results with all geotextiles. The goal of polymer research should be to find a polymer that causes the slurry of rock crushing fines to

quickly flocculate which opens up drainage paths for the water so the rock crushing fines will dewater more quickly.

6.3 Predicting geotextile filtration performance

Determining a suitable parameter to predict the filtration performance of rock quarry fines and geotextile tubes would decrease the amount of time usually allotted for selecting a geotextile to filter a soil. Recent studies by Koerner and Koerner (2006), Moo-Young et al. (2002), Aydilek and Edil (2002), and Liao and Bhatia (2005) have shown that typical parameters used to predict filtration with geotextiles, such as AOS, O_{95} , O_{50} , or ratios such as O_{95}/D_{85} are not suitable for predicting filtration behavior of geotextiles with fine grained material. Therefore, comparing results of bubble point tests of geotextiles, gradation testing of fine grained materials, and hanging bag tests would be beneficial in determining a suitable parameter or parameters to predict geotextile filtration performance with rock crushing fines.

References

Allaby, A and Allaby, M., (1999) "coefficient of consolidation." A Dictionary of Earth Sciences, *Encyclopedia.com*. 2 Dec. 2009, <http://www.encyclopedia.com>

ASTM Standard D 422, (2007) Test Methods for Particle-Size Analysis of Soils, *Annual Book of ASTM Standards*, ASTM International, West Conshohocken, PA.

ASTM Standard D 854, (2007) Test Methods for Specific Gravity of Soil Solids by Water Pycnometer, *Annual Book of ASTM Standards*, ASTM International, West Conshohocken, PA.

ASTM Standard D 1252, (2007) Test Methods for Uncompacted Void Content of Fine Aggregate (as Influenced by Particle Shape, Surface Texture, and Grading), *Annual Book of ASTM Standards*, ASTM International, West Conshohocken, PA.

ASTM Standard D 4318, (2007) Test Methods for Liquid Limit, Plastic Limit, and Plasticity Index of Soils, *Annual Book of ASTM Standards*, ASTM International, West Conshohocken, PA.

ASTM Standard D 4355, (2007) Test Methods for Deterioration of Geotextiles by Exposure to Light, Moisture and Heat in a Xenon Arc Type Apparatus, *Annual Book of ASTM Standards*, ASTM International, West Conshohocken, PA.

ASTM Standard D 4491, (2007) Test Methods for Water Permeability of Geotextiles by Permittivity, *Annual Book of ASTM Standards*, ASTM International, West Conshohocken, PA.

ASTM Standard D 4595, (2007) Test Methods for Tensile Properties of Geotextiles by the Wide-Width Strip Method, *Annual Book of ASTM Standards*, ASTM International, West Conshohocken, PA.

ASTM Standard D 4751, (2007) Test Methods for Determining Apparent Opening Size of a Geotextile, *Annual Book of ASTM Standards*, ASTM International, West Conshohocken, PA.

ASTM Standard D 4884, (2007) Test Methods for Strength of Sewn or Thermally Bonded Seams of Geotextiles, *Annual Book of ASTM Standards*, ASTM International, West Conshohocken, PA.

ASTM Standard D 5101, (2007) Test Methods for Measuring the Soil-Geotextile Stem Clogging Potential by the Gradient Ratio, *Annual Book of ASTM Standards*, ASTM International, West Conshohocken, PA.

ASTM Standard D 5158, (2007) Test Methods for Determination of Particle Size of Powdered Activated Carbon by Air Jet Sieving, *Annual Book of ASTM Standards*, ASTM International, West Conshohocken, PA.

ASTM Standard D 6767, (2007) Test Methods for Pore Size Characteristics of Geotextiles by Capillary Flow, *Annual Book of ASTM Standards*, ASTM International, West Conshohocken, PA.

API Filter Press Instruction Manual, Series 300, (2009)
<http://www.expotechusa.com/manuals%5Cfann/30001.pdf>

Aydilek, A.H., Edil, T.B., (2002) “Filtration Performance of Woven Geotextiles with Wastewater Treatment Sludge”, *Geosynthetics International Vol. 9 No. 1*, 41 – 69

Aydilek, A.H., Oguz, S.H., and Edil, T.B., (2005) “Constriction Size of Geotextile Filters” *Journal of Geotechnical and Geoenvironmental Engineering, ASCE, Vol. 131, No. 1*, 28-38

Ben Meadows, (2009),
<http://www.benmeadows.com/search/Field+Scout/+647/22441/134687/?isredirect=true>

Cantre, S., (2002) “Geotextile Tubes – Analytical Design Aspects” *Geotextiles and Geomembranes, Vol. 20, No. 5*, 305 – 319

Elton, D.J., Hayes, D.W., and Adanur, S. (2007) “Bubblepoint Testing of Geotextiles: Apparatus and Operation” *Geotechnical Testing Journal, Vol. 30, No. 1*, 1-8

EPA, (2000) “Biosolids Technology Fact Sheet Belt Filter Press”

Georgia Tech Aggregate Properties, (2009)
<http://people.ce.gatech.edu/~kk92/labs/agglab.doc>

Gregory, A.S., Whalley, W.R., Watts, C.W., Bird, N.R.A., Hallett, P.D., Whitmore, A.P. (2005), “Calculation of the compression index and precompression stress from soil compression test data” *Soil and Tillage Research, Vol. 89, No. 1*, 45-57

Han, Jie, (2009) “Designing Geosynthetics for Separation, Filtration, and Drainage” Class notes,
http://www.engr.ku.edu/~jhan/CE889_2009.htm

Huang, C.C., Luo, S.Y., (2007) “Dewatering of Reservoir Sediment Slurry Using Woven Geotextiles. Part I: Experimental Results” *Geosynthetics International, Vol 14, No. 3*, 253 – 263

Koerner, G.R., Koerner, R.M., (2005) “Geotextile Tube Assessment Using a Hanging Bag Test” *Geotextiles and Geomembranes, Vol. 24, No. 2*, 129 – 137

Koerner, R.M., (2005) *Designing With Geosynthetics 5 ed.* Prentice Hall Upper Saddle River, NJ

Kutay, M.E., Aydilek, A.H., (2005) “Filtration Performance of Two-Layer Geotextile Systems” *Geotechnical Testing Journal*, Vol. 28, No. 1, 1 – 13

Kutay, M.E., Aydilek, A.H., (2003) “Hydraulic Compatibility of Geotextile Drains with Fly Ash in Pavement Structures” *Presented at the 82nd Annual Meeting of the Transportation Research Board, Washington D.C., 2003*

Kutay, M.E., Aydilek, A.H., and Hussein S., (2005) “Dewatering Fly Ash Slurries using Geotextile Containers” *GRI-18 Geosynthetic Research and Development in Progress*, 4271-4277

Liao, K., Bhatia, S.K., (2005) “Geotextile Tube: Filtration Performance of Woven Geotextiles Under Pressure” *Geosynthetics '05, IFAI Las Vegas, Nevada*, 15 p

Luetlich, S.M., Giroud, J.P., Bachus, R.C., (1992) “Geotextile Filter Design Guide” *Geotextiles and Geomembranes*, Vol. 11, No. 4-6, 355 – 370

Merriam-Webster (2009) Mafic
<http://mw1.merriam-webster.com/dictionary/mafic>

Moo-Young, H., Gaffney, D., Mo, X. (2002) “Testing Procedures to Assess the Viability of Dewatering with Geotextile Tubes” *Geotextile and Geomembranes*, Vol. 20, No. 5, 289-303

Muthukumar, A.E., Ilamparuthi, K., (2006) “Laboratory Studies on Geotextile Filters as used in Geotextile Tube Dewatering” *Geotextiles and Geomembranes*, Vol. 24, No. 4, 210 – 219

Palmeira, E.M., Gardoni, M.G., (2000) “The Influence of Partial Clogging and Pressure on the Behavior of Geotextiles in Drainage Systems” *Geosynthetics International*, Vol. 7, No. 4, 403 - 431

Pavement Interactive, (2009) Fine Aggregate Angularity,
http://pavementinteractive.org/index.php?title=Fine_Aggregate_Angularity

Professional Equipment, (2009),
http://www.professionalequipment.com/product_images/134689_probe-rods.jpg

Shin, E.C., Oh, Y.I., (2007) “Coastal erosion prevention by geotextile tube technology” *Geotextiles and Geomembranes*, Vol. 25, No. 4-5, 264-277

Soil Water Content Sensors and Measurement, (2009),
<http://www.sowacs.com/sensors/tdr.html>

Standard Methods 2120 B, 1992: Visual Comparison Method, *Standard Methods for the Examination of Water and Wastewater*, American Public Health Association, Washington D.C.

Standard Methods 2130 A, 1992: Turbidity, *Standard Methods for the Examination of Water and Wastewater*, American Public Health Association, Washington D.C.

Standard Methods 2540 D, 1992: Total Suspended Solids Dried at 103 - 105°C, *Standard Methods for the Examination of Water and Wastewater*, American Public Health Association, Washington D.C.

University of Maine, (2009), Atterberg Limits,
http://www.civil.umaine.edu/cie366/atterberg_limits/default.htm

USGS, (2007). Minerals Yearbook [Advance Release]. United States Geological Service.
http://minerals.usgs.gov/minerals/pubs/commodity/stone_crushed/myb1-2007-stonc.pdf

USGS (2009) Biotite Gneiss
<http://tin.er.usgs.gov/geology/state/sgmc-lith.php?text=biotite+gneiss>

Venkatramaiah, C. (2006) Geotechnical Engineering,
New Age International Publishers pg 134

Vulcan Materials (2009) Barin Quarry Product Specifications
<http://www.vulcanmaterials.com/vcm/productspecs.asp?fac=170>

Worley, J.W., Bass, T.M., and Vendrell, P.F., (2004) “Field Test of Geotextile Tube for Dewatering Dairy Lagoon Sludge.” *Proceedings of 2004 ASAE/CSAE Annual International Meeting, Paper number 044078*, August 2004

Appendix 1: Graphs from Consolidation Tests

Consolidation dial reading vs time graphs for stress increments of 11.97, 23.94, 47.88, 95.76, 191.52, 383.04, 766.08, and 1532.16 kPa applied stress.

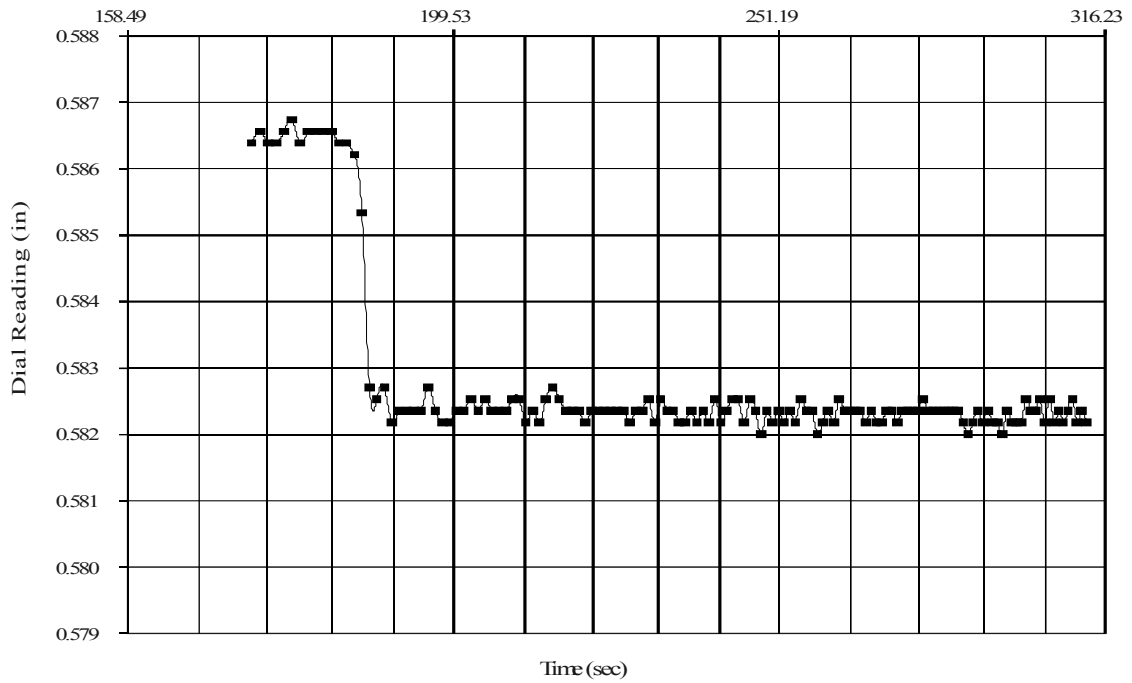


Figure 40: Consolidation dial reading vs time for 11.97 kPa applied stress

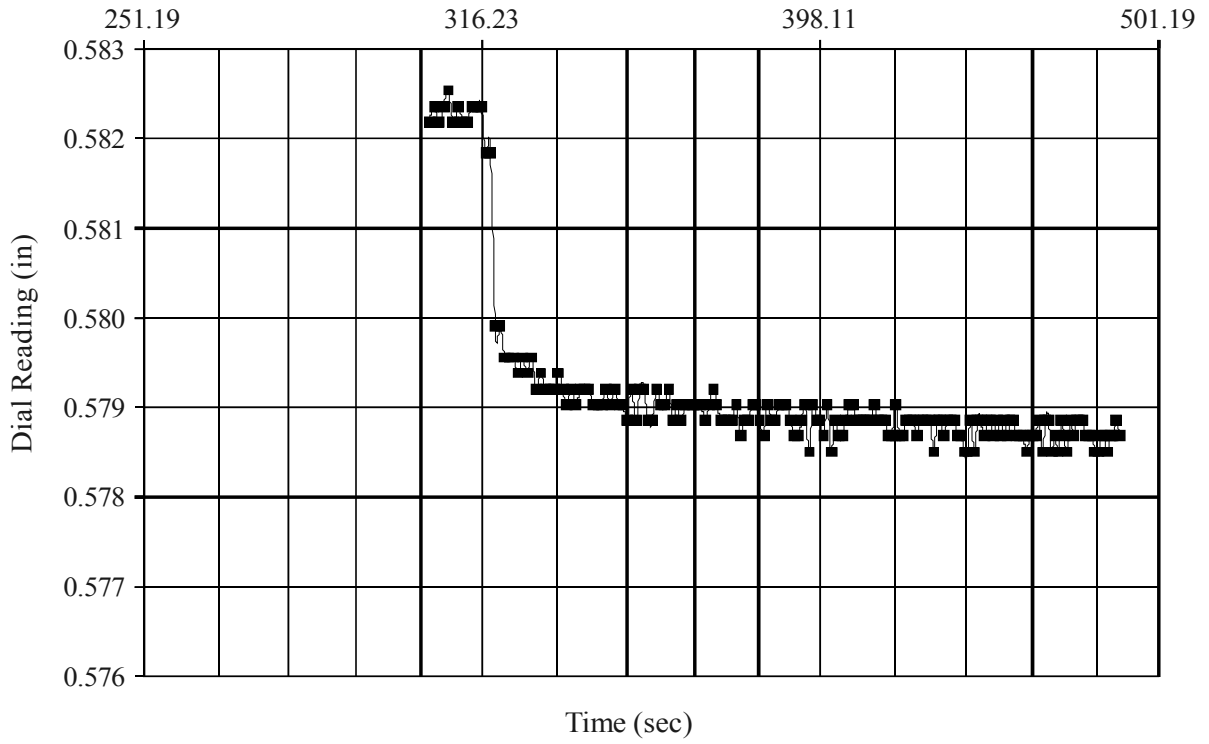


Figure 41: Consolidation dial reading vs time for 23.94 kPa applied stress

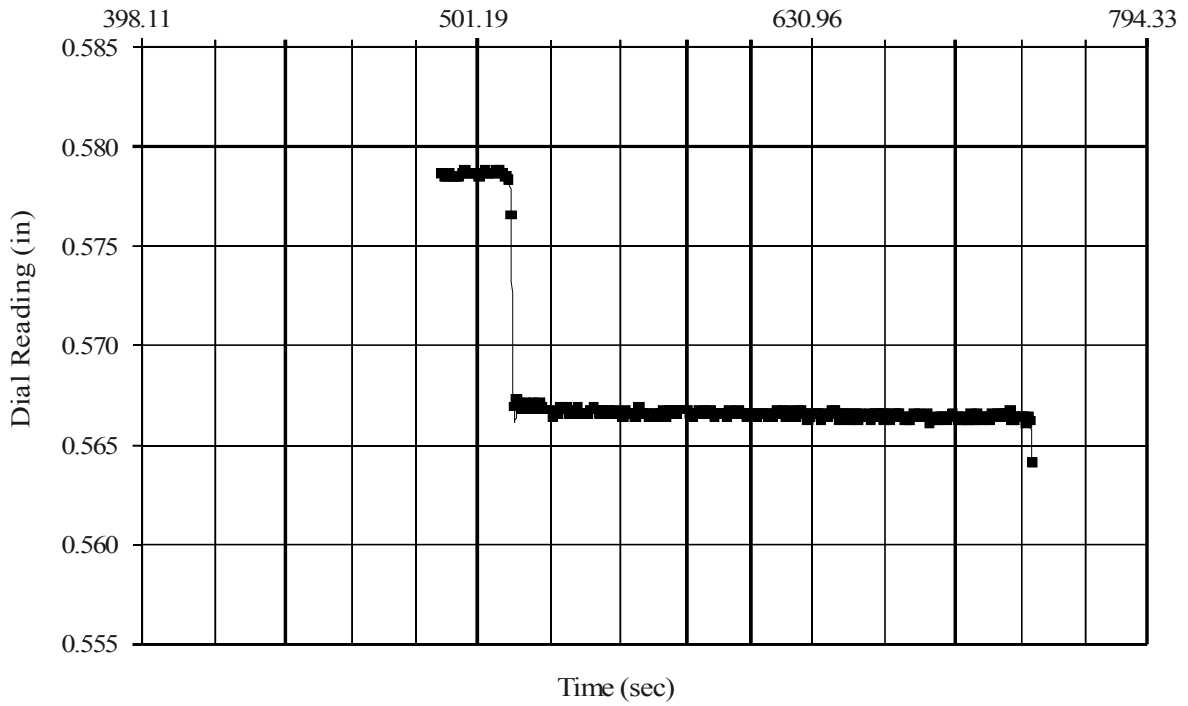


Figure 42: Consolidation dial reading vs time for 47.88 kPa applied stress

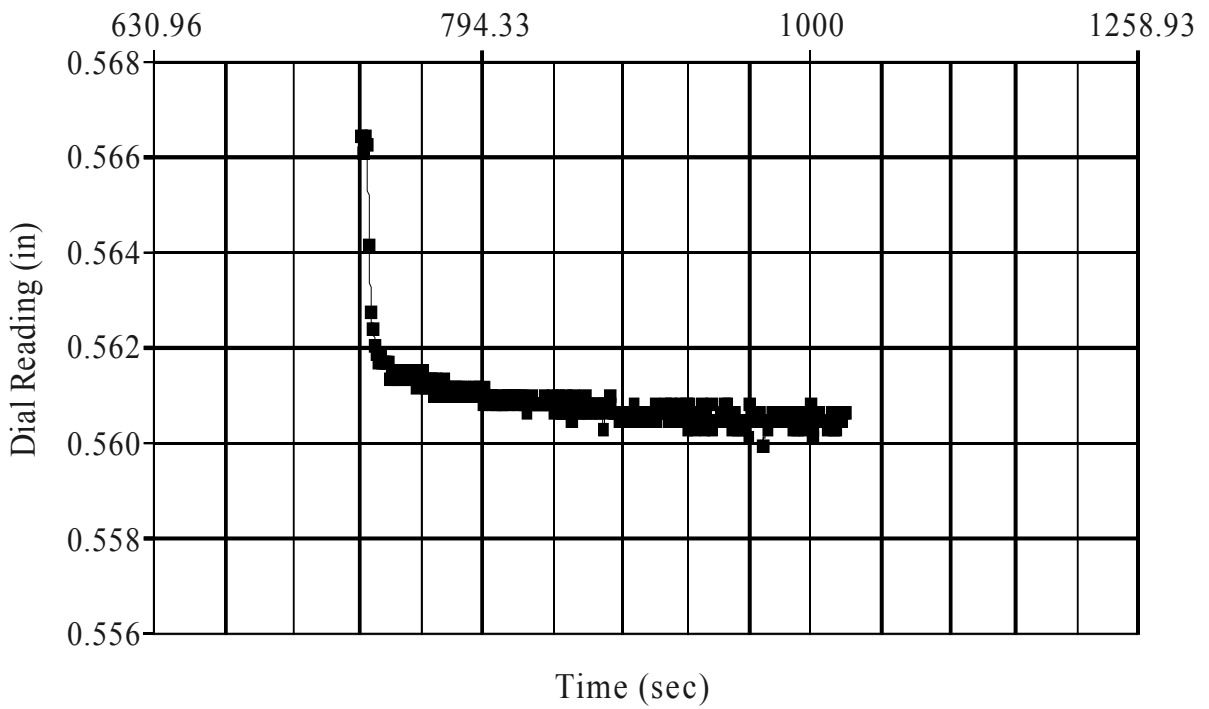


Figure 43: Consolidation dial reading vs time for 95.76 kPa applied stress

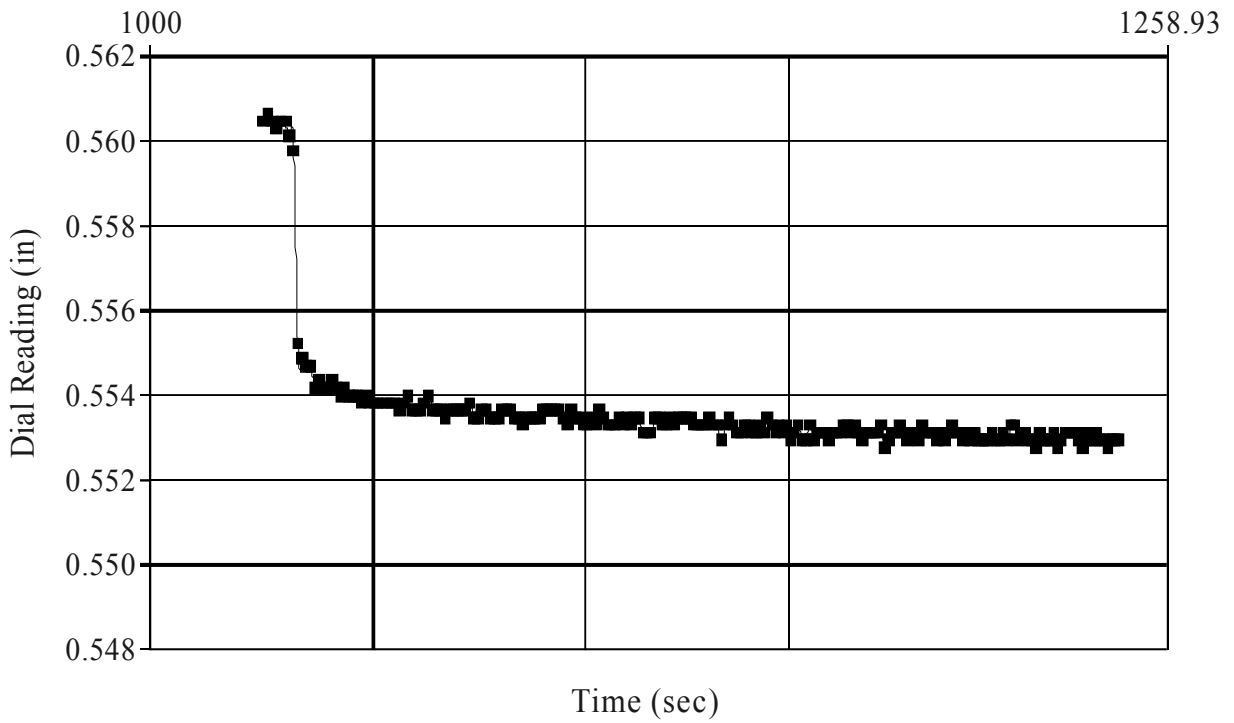


Figure 44: Consolidation dial reading vs time for 191.52 kPa applied stress

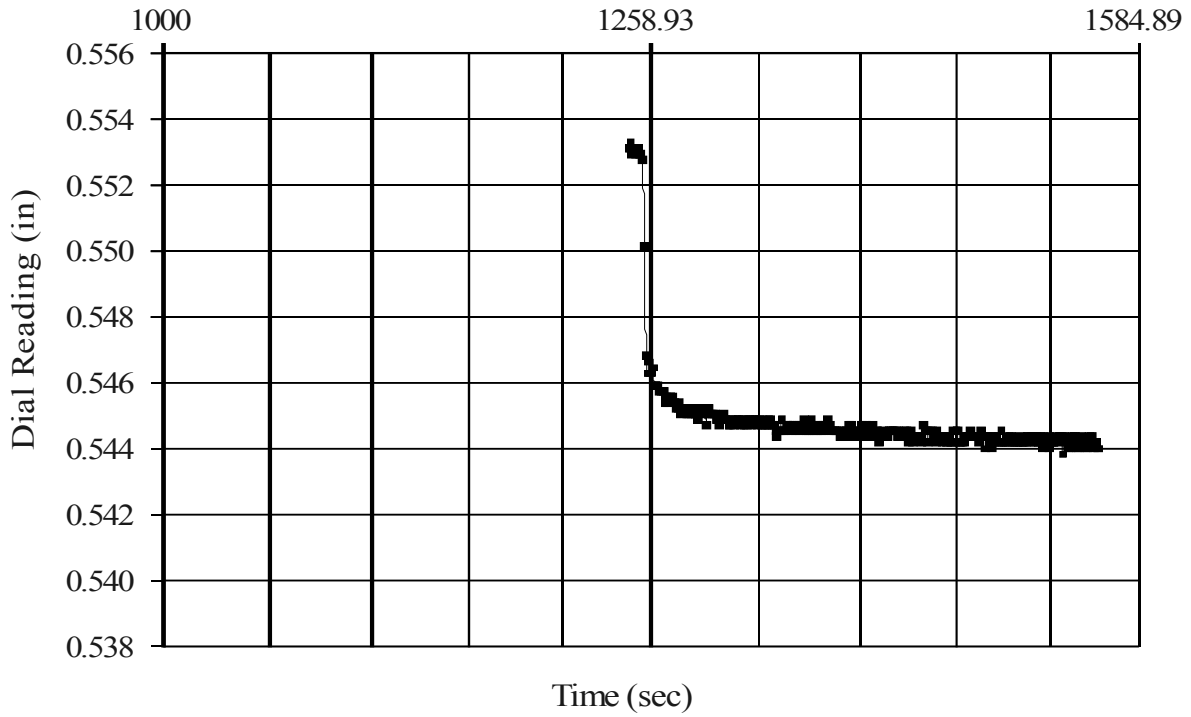


Figure 45: Consolidation dial reading vs time for 383.04 kPa applied stress

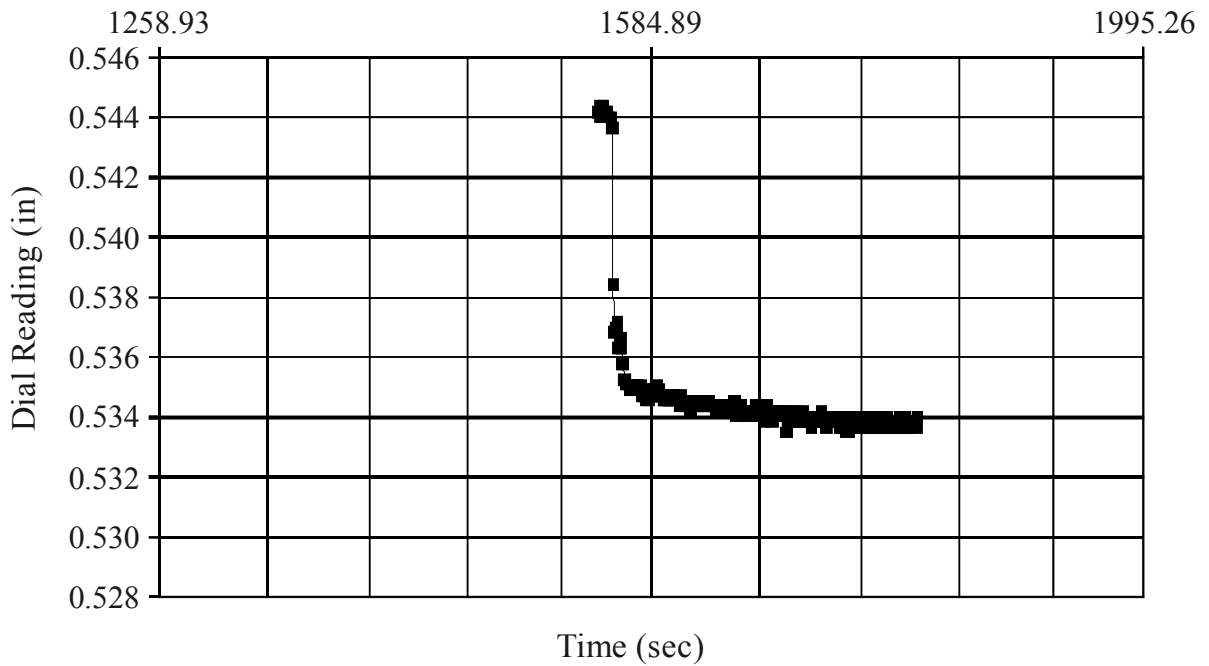


Figure 46: Consolidation dial reading vs time for 766.08 kPa applied stress

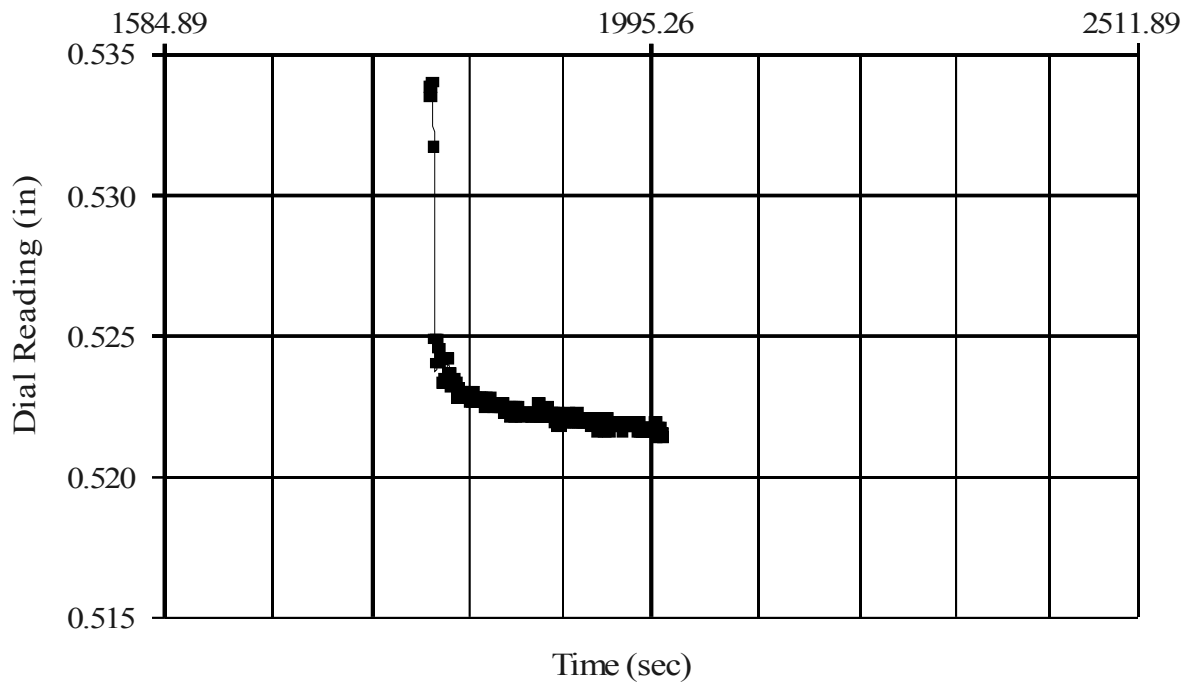


Figure 47: Consolidation dial reading vs time for 1532.16 kPa applied stress

Appendix 2: Chemical composition of polymers

Solve # 153	Anionic Polyacrylamide Copolymer
Petroleum Distillate	22.4%
Alcohols (C10-16) Ethoxylated	0-2.6%
Alcohols (C12-14) Ethoxylated	0-2.6%
Alcohols (C12-16) Ethoxylated	0-2.6%
Solve # 154	30 Mole % Anionic Polyacrylamide in Water-in-Oil Emulsion
Petroleum Distillate	20.5-22.5%
Alcohols (C10-16) Ethoxylated	0-2.7%
Alcohols (C12-14) Ethoxylated	0-2.7%
Alcohols (C12-16) Ethoxylated	0-2.7%
Solve # 163	Anionic Polyacrylamide
Petroleum Distillate	20-35%
Alcohols (C10-16) Ethoxylated	0-3.6%
Alcohols (C12-14) Ethoxylated	0-3.6%
Alcohols (C12-16) Ethoxylated	0-3.6%
Ethoxylated Oleylmine	0-3%
Solve # 2250A	Water Soluble Polymer in Emulsion
Identification of the Preparation	
Anionic Water Soluble Polymer in Emulsion	
Solve # 9310	Anionic Emulsion Polymer
2-Propenoic Acid, Sodium Salt, Polymer with 2-Propenamide	30-40%
Petroleum Distillates	20-30%
Poly(Oxy-1, 2-Ethanedily, α -(4-Nonylphenol)- ω -Hydroxy-, Branched	1-3%
Solve # 9350	Anionic Emulsion Polymer
2-Propenoic Acid, Sodium Salt, Polymer with 2-Propenamide	60-70%
Petroleum Distillates	20-30%
Poly(Oxy-1, 2-Ethanedily, α -(4-Nonylphenol)- ω -Hydroxy-, Branched	1-3%

Table 21: Chemical Composition of Polymers provided by WaterSolve, LLC